12-2005

Kinetics of Cellulose Dissolution in N-Methyl Morpholine-N-Oxide and Evaporative Processes of Similar Solutions

John William Tierney
University of Tennessee - Knoxville

To the Graduate Council:

I am submitting herewith a thesis written by John William Tierney entitled "Kinetics of Cellulose Dissolution in N-Methyl Morpholine-N-Oxide and Evaporative Processes of Similar Solutions." I have examined the final electronic copy of this thesis for form and content and recommend that it be accepted in partial fulfillment of the requirements for the degree of Master of Science, with a major in Chemical Engineering.

John R. Collier, Major Professor

We have read this thesis and recommend its acceptance:

Billie J. Collier, Simion Petrovan, Timothy G. Rials

Accepted for the Council:
Carolyn R. Hodges

Vice Provost and Dean of the Graduate School

(Original signatures are on file with official student records.)

To the Graduate Council:

I am submitting herewith a thesis written by John William Tierney entitled "Kinetics of Cellulose Dissolution in N-Methyl Morpholine-N-Oxide and Evaporative Processes of Similar Solutions." I have examined the final electronic copy of this thesis for form and content and recommend that it be accepted in partial fulfillment of the requirements for the degree of Master of Science, with a major Chemical Engineering.

John R. Collier
Major Professor

We have read this thesis and
recommend its acceptance:

Billie J. Collier

Simion Petrovan

Timothy G. Rials

Accepted for the Council:

Anne Mayhew
Vice Chancellor and
Dean of Graduate Studies

(Original signatures are on file with official student records)

Kinetics of Cellulose Dissolution in N-Methyl Morpholine-N-Oxide and Evaporative Processes of Similar Solutions

A Thesis presented for the Master of Science Degree

The University of Tennessee, Knoxville

John William Tierney

December 2005

Dedication

This thesis is dedicated to Melinda, for always believing in me and for her unwavering love, support, and encouragement.

Abstract

The lyocell process is an environmentally friendly process for producing regenerated cellulose fibers, but is not entirely understood. The lyocell process uses the hygroscopic solvent N-methyl morpholine N-oxide (NMMO) to dissolve cellulose; the resulting solution is often termed a lyocell solution [1-4]. It is the objective of this study to better understand the process by which cellulose dissolves and the nature of lyocell solutions. By observing the disappearance of cellulose fibers into the solvent, rate data may be obtained from which kinetic parameters may be developed. Additionally an independent method for determining the concentration of cellulose in lyocell solutions was desired so as to better to gauge the effect of concentration on the behavior of the solution.

Water affects the behavior of NMMO, making it an important factor in the lyocell process. The water content in lyocell samples may be determined by a number of methods including NMR spectroscopy and Fischer's method. Unfortunately, these methods each require additional chemicals that add to the cost of the analysis. Therefore a novel method was sought for determining the water content of lyocell samples without the use of additional chemicals.

Samples of NMMO, some containing dissolved cellulose, were subjected to thermogravimetric analysis on a Pyris 1 TGA to observe the evaporative process and note any effects of cellulose on that process in an effort to develop a rudimentary approach to determining water content on lyocell samples.

Additionally, the dissolution of cellulose into NMMO was observed under a Fourier Transform Infrared Spectrometer and a light microscope. Digital photographs

with corresponding time measurements were taken of the dissolving cellulose that resulted in dissolution data for single fibers. This was done at several temperatures to extract rate constants for the dissolution process.

The results of this project confirmed that cellulose depresses the melting point of NMMO monohydrate and led to a novel method for determining water content in lyocell samples. Detailed mid-infrared spectra were collected for cellulose, NMMO monohydrate, and lyocell samples which were used to develop a predictive model for determining cellulose content in lyocell solutions. Finally, the temperature and surface area dependence for the process of cellulose dissolution in NMMO monohydrate were demonstrated and a rate constant and Arrhenius parameters for the process were obtained.

An examination of the phase behavior of NMMO at the onset of cellulose solubility would aid in understanding the dissolution process as would a DSC analysis of NMMO crystallization versus water content. A more detailed multivariate analysis of mid-infrared spectra from lyocell solutions may be performed in the future to improve the predictive model.

Table of Contents

Section

List of Tables

Table

List of Figures

Figure

1. Justification and Objectives

The viscose process has traditionally been the chief method for the production of regenerated cellulose fibers in the United States. The lyocell process is an environmentally friendly alternative process currently in production, but is not entirely understood. The lyocell process uses the hygroscopic solvent N-methyl morpholine N-oxide (NMMO) to dissolve cellulose; the resulting solution is often termed a lyocell solution [1-4]. It is the objective of this study to better understand the process by which cellulose dissolves and the nature of lyocell solutions. By observing the disappearance of cellulose fibers into the solvent, rate data may be obtained from which kinetic parameters may be developed.

Fourier Transform Infrared (FTIR) Spectroscopy is a valuable tool in the analysis of chemical compounds, but such data is not widely available for NMMO. This study obtains mid-infrared spectra for NMMO and utilizes an FTIR analysis on a variety of lyocell solutions. Additionally an independent method for determining the concentration of cellulose in lyocell solutions was desired so as to be better able to gauge the effect of concentration on the behavior of the solution.

Due to the hygroscopic nature of NMMO and water's effect on its behavior, knowing the water content in lyocell samples is important. Many of the methods available for water content determination require additional chemicals that add to the cost of the analysis [2, 5-9]. Therefore a novel method was sought for determining the water content of lyocell samples without the use of additional chemicals.

2. Introduction

A. History of Lyocell

The employment of cellulose in society dates back to ancient Egypt, and has been used extensively in the last one hundred years for the production of fibers for textiles and other materials. The growing importance of cellulose fibers is realized not only in its mechanical properties, but also in the fact that cellulose is biocompatible and a renewable resource. These very significant features indicate that the demand for cellulose fibers is not likely to subside [1, 10]. For many years in the United States cellulose fibers were generally made on an industrial scale exclusively through a viscose process that required derivatization of cellulose pulps before cellulose could be dissolved and processed to form regenerated cellulose fibers. Unfortunately this viscose process had low productivity, was energy intensive, and made use of heavily regulated, environmentally harmful chemicals such as carbon disulfide [2].

In the past several decades, an innovative technology has come to light as a more environmentally friendly alternative to the viscose process. Unlike the viscose process, derivatization of cellulose is not required. Instead cellulose can be dissolved directly by water mixed with the nontoxic, biodegradable amine oxide NMMO. Additionally, the amine oxide can be almost completely recovered and recycled. In the 1980s several companies researched this process and developed brand names for their products. One such company chose the name Lyocell® for their fibers. The term lyocell is now generally applied to both the process, the cellulose fibers it produces, and mixtures of NMMO and cellulose. Several pilot and full-scale plants across Europe, Asia, and the United States now use the lyocell process to produce cellulose fibers [1, 3-4, 11-12].

B. Properties of the Solvent

N-methyl morpholine N-oxide is a six-membered ring that is aliphatic and contains a highly polar N-O group, as well as an oxygen on the opposite side of the ring from the nitrogen (Figure 1). The highly polar N-O bond found in NMMO makes for excellent water solubility and gives the molecule the ability to form hydrogen bonds. NMMO is also highly oxidative and can degrade with explosive results if given the opportunity through a catalyst or heating to 180-185 ºC, which is the approximate melting point of the anhydrous form [1, 2, 5, 8].

There are three forms of NMMO: anhydrous, monohydrate, and disesquihydrate that has 2.5 molecules of water for each molecule of NMMO. While it is possible to have a hydration number (n) other than zero, one, or two and a half, the composition is then some combination of the three stable forms mentioned. At room temperature all three hydrates are also extremely hygroscopic, but with heating this behavior is reversed and water evaporates from the NMMO. The pure anhydrous form cannot be obtained by simple evaporative methods, but rather requires the use of organic solvents and crystallization or vacuum sublimation [1, 2, 5, 8].

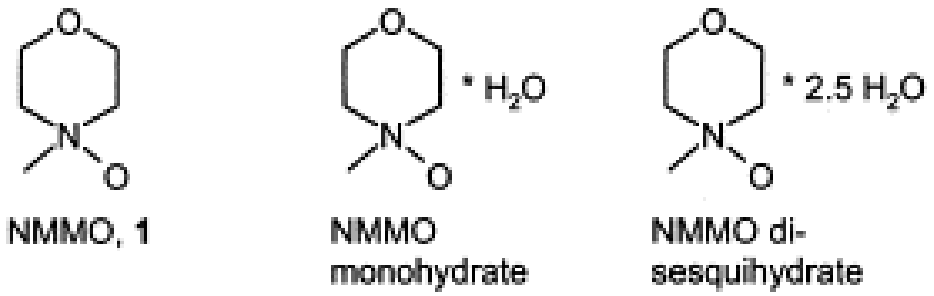

Figure 1: NMMO and its hydrates [1].

It should also be noted that the crystal structure of NMMO differs depending on the hydration number (Figure 2) [1, 6-7]. If NMMO is in one of the pure hydrated forms (n = 0, 1, 2.5) then it exists as only one kind of crystal; however at any other hydration number, there is a mixture of the crystal forms [6, 8]. Additionally, research has shown cellulose depresses the melting point of NMMO and disrupts its crystal structure [2, 6, 8]. Since NMMO is a flexible six-membered ring, the ability to shift between several conformations in solution might be expected. It has been determined by Rosenau, et. al. [4] that five conformations—two boat, one twist, and two chair conformations—do exist for NMMO in solution. However, only the chair conformations are energetically favorable enough to ever be present in any appreciable amount. It was noted that there is a preference for the chair conformation with an axial oxygen. This preference diminished as the solvent became increasingly more polar due to increased interactions with the solvating material. The increase in the prevalence of the equatorial oxygen, which is slightly less energetically favorable than an oxygen in the axial position, is likely due to the stabilizing effect a polar solvent may have by forming hydrogen bonds with NMMO. In order to determine the conformation NMMO might take on in the presence of cellulose, the sugar cellobiose was added to a 0.1 molar solution of NMMO in water. Interestingly, the chair conformation with an equatorial oxygen disappeared and only the conformations with axial orientations were found, despite the fact that in water alone nearly 25% of the NMMO was found to be in the equatorial conformation [4]. This interaction affecting the NMMO conformation seems to support the proposed model of cellulose-NMMO interaction in the dissolution of cellulose discussed by other researchers (Figure 3) [13-14].

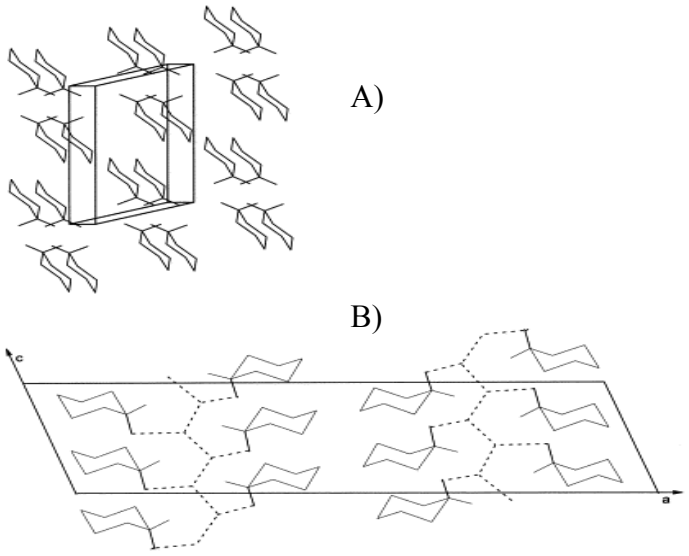

Figure 2: NMMO crystal structures. A) Anhydrous NMMO B) NMMO Monohydrate [1].

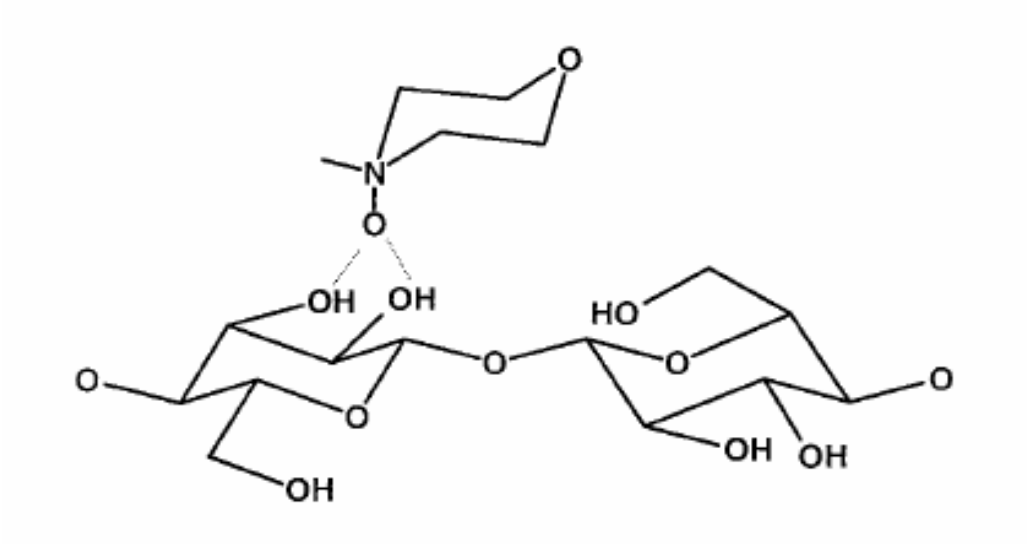

Figure 3: Possible orientation of NMMO relative to cellulose in solution [13].

C. Importance of Water

The water content of NMMO is plainly an important factor in NMMO behavior, even affecting melting point (Table 1). Water content in NMMO can be determined quantitatively by using Fischer's titration method or NMR spectroscopy, which requires the use of deuterated solvents [2, 5-6, 8]. In addition, Laity et. al. [15] used magnetic resonance imaging (MRI) to study the coagulation of cellulose from NMMO. Composition changes for NMMO and water in a cellulose-NMMO gel could be detected using the MRI despite some resolution issues [15]. MRI could then also be used to determine the hydration number of NMMO as a solvent prior to its use as a cellulose solvent. Perhaps more significantly, however, MRI might also allow the observation of the dissolution process itself.

The polarity of NMMO and its ability to form hydrogen bonds is a key factor in its ability to dissolve cellulose. It has been noted, however, that the water content is also an important factor in cellulose dissolution in NMMO because the water and cellulose effectively compete for hydrogen bond spots and water, being smaller and more mobile, wins out. For this reason when the hydration number is 2.5 it is understandable why NMMO cannot dissolve cellulose—all of the slots for hydrogen bonds have already been filled. In fact, for NMMO to be able to dissolve cellulose, the water content needs to be approximately 16 wt% or less, which falls between the disesquihydrate and monohydrate forms (Table 1) [1, 2, 8, 14-15].

D. Theories of Dissolution

Although it is in production, the lyocell process is not completely understood—in particular the molecular processes during solvation remain unidentified. Theoretically

Table 1: Water content and melting point data for NMMO hydrates [8].

Form of NMMO	n	Wt. % Water	Melting Point
Anhydrous	0	0	184ºC
Monohydrate	1	13.3	78ºC
Disesquihydrate	2.5	27.8	39ºC

the dissolution of cellulose into the NMMO/water mixture should be a physical process where the NMMO disrupts the intermolecular and intramolecular hydrogen bonds cellulose forms with itself. As the hydrogen bonds of cellulose are broken, new ones form between NMMO and cellulose to form a molecular complex. The steps for a mechanism describing this process have not yet been determined [1, 3, 4, 7-8]. It appears there is more than just the breaking and forming of hydrogen bonds occurring, though. The presence of chromophores in lyocell solutions has been detected and may even be observed with the eye in larger quantities as causing a yellowing of lyocell fibers. These chromophores are the result of side reactions that occur due to the oxidative nature of NMMO and the temperatures at which the process is carried out. They have been shown to be the result of degradation and condensation reactions of monosaccharides. The monosaccharides, consequently, are the result of the degradation of cellulose. Researchers continue to search for the mechanism that leads from the cellulose to the monosaccharides [3, 16].

It has been hypothesized that the solvation process occurs in two stages. First the more accessible cellulose areas dissolve with simultaneous swelling, and then the crystalline regions go into solution [17]. This hypothesis is supported by the work of Petrovan, et. al. [17] who prepared lyocell solutions from dissolving pulps with average

degrees of polymerization (DP) of 670 and 1720. The pulp and NMMO-monohydrate were mixed in a Haake Torque Rheometer Rheocord H90 at 60 RPM and 90 ºC for two hours. Solutions with an average DP of 670, 932, 1195, 1457, and 1720 were made (Table 2). During mixing the torque on the rotors was recorded versus time. A plot of these data can be seen in Figure 4, which shows a brief period of initial low torque that could correspond to the solvation of the more accessible regions and lower DP chains. Simultaneously, swelling of the cellulose occurs, and upon its dissolution there is a viscosity increase in the solution resulting in a need for increased torque. Upon attainment of a steady state value for the torque, the solvation process may be considered complete. One may also note from the plot that the total amount of torque required for solvation increases with increasing DP [17]. The most interesting curve is perhaps that for the dissolution of the DP 1457 pulp. It is the blend of the 75 percent DP 1720 and 25 percent DP 670 raw pulps and exhibits an initial torque increase to about 1.25 Nm and then another several minutes later to about 1.75 Nm. This could be due to the swelling and dissolution of the lower DP component, followed by the dissolution of the higher DP component. This would further validate the hypothesis that lower DP and more accessible regions dissolve first, while the higher DP chains and less accessible domains are swollen and subsequently penetrated and dissolved by the NMMO. The hypothesis put forth by Petrovan, et. al. is supported by Kim, et. al. [2] who also note a swelling process followed by solvation when the hydration number (n) of NMMO is less than 1.65 (where n = 1 for NMMO monohydrate). However, even once dissolved, it has been shown that the cellulose is not molecularly dispersed in the solvent, but rather present in aggregates throughout the solvent [1].

Table 2: Composition data for lyocell solutions used by Petrovan, et. al.

Avg. DP	DP 670	DP 1720
670	100%	0%
932	75%	25%
1195	50%	50%
1457	25%	75%
1720	0%	100%

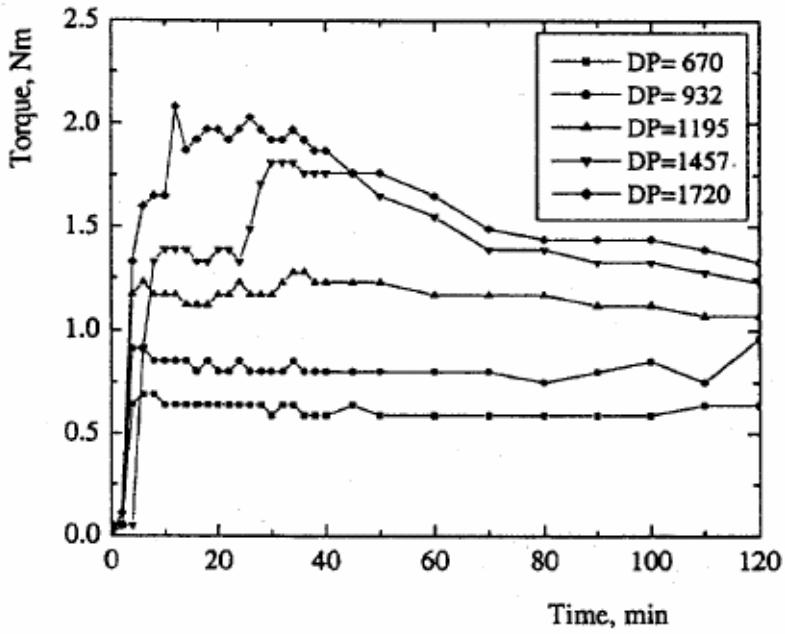

Figure 4: Variation of the rotors torque in the course of lyocell solutions preparation [17].

With the advancement of computer technology, it has become easier to model molecular interactions. Kast, et. al. [18] used a molecular dynamics simulation technique to better understand the interactions between NMMO and water. The researchers modeled 440 molecules in an equimolar mixture at 1 bar and 373.15 K – a temperature commonly used for industrial scale cellulose processing. The simulation showed the development of solvent shells around the oxygens in NMMO, particularly the oxygen bound to the nitrogen. These solvent shells amount to multiple water molecules being within the immediate vicinity of the oxygen of interest. There is also some indication that a water molecule is located above the morpholine ring and interacts with both oxygens [18]. The weak interaction of the second oxygen with water and the interaction of a water across the ring would help explain the hydration number of 2.5 for a fully hydrated NMMO molecule. Kast et. al. [18] also qualitatively examined the effect of flexibility on solvation and noted that it likely plays a role in dissolving cellulose because a similar, less flexible amine oxide does not dissolve cellulose. Additionally, the authors cite another work [13] that also indicates the importance of flexibility when NMMO dissolves cellulose and describes a possible orientation for NMMO relative to cellulose in a solvated system, as previously shown in Figure 3.

E. Analytical Methods

Differential scanning calorimetry is a method of determining thermodynamic properties of compounds. A differential scanning calorimeter (DSC) applies heat to a compound in a DSC cell in a precise manner and records the amount of heat applied and the temperature of the sample. Using this information the temperature at which phase transitions occur may be determined.

A thermogravimetric analyzer records the weight and temperature of a sample versus time. The temperature of the sample may be raised at a given rate to observe the degradation temperature of a material or the temperature may be held at a particular value to drive off a component, such as water, to determine the composition of a mixture or solution.

Fourier Transform Infrared Spectroscopy is a tool that is often used to examine chemical compounds because different compounds absorb infrared radiation at different wavelengths. An FTIR spectrometer measures transmission of infrared radiation through a material, which is then converted within the software to absorbance data. Absorbance data is obtained along the 700-4000 wavelength spectrum in intervals specified by the user. The absorbance data is displayed graphically as an absorbance spectrum with peaks indicating the wavelengths the material strongly absorbs.

A principle component analysis (PCA) examines statistically significant portions of a data set and groups samples based on similarities. In the case of a set of absorbance spectra, a PCA examines the peaks and valleys in the spectra to develop clusters of samples that have the most similar spectra. A projection of latent structures (PLS) examines statistically significant portions of data, whose samples have known groupings, for differences in samples and develops a predictive model based on those differences. Typically, two-thirds of a data set is used to develop, or calibrate, the model. The model is then validated by applying it to the remaining one third of the data to see if the properties of the data can be correctly predicted. The Unscrambler® software has the capability to examine and group samples based on their spectra and is the software tool

used in this project for PCA and PLS. The software also recognizes outliers and gives the user the option to eliminate them from the analysis.

When studying chemical processes, it is often useful to know the reaction rate constant, pre-exponential factor, and activation energy. This information may be readily obtained from a reaction rate experiment to which the method of initial rates is applied as described by Fogler [19] and summarized here. The concentration of a key reactant is measured at a specific temperature against time during a reaction. The initial reaction rate may then be obtained for each concentration by measuring the slope of the concentration versus time curve over the first few data points. In order to obtain the rate constant, the experiment must be run several times with varying initial concentrations and constant temperature. If the rate law for the reaction is in the form shown in Appendix A, the natural log of the rate constant is the intercept of a plot of the natural log of the initial reaction rate versus the natural log of the initial concentration. The pre-exponential factor and activation energy for the process are obtained by applying the method of initial rates to concentration versus time data acquired at two additional temperatures. The natural log of the three rate constants may then be plotted against the inverse of the absolute temperature at which the measurements were taken. The resulting plot has an intercept equal to the natural log of the pre-exponential factor and a slope of the negative activation energy divided by the ideal gas constant.

F. Methods of Lyocell Preparation

When mixing a cellulose-NMMO solution there are two predominant approaches: the evaporative and direct methods. In the evaporative method cellulose is added to NMMO with a hydration number of approximately 1.65 or greater. The excess water is

then evaporated until the hydration number is approximately one. Although this method does provide a homogenous solution, it takes a long time and can result in degradation of the NMMO and cellulose due to the extended times at elevated temperatures [2].

Perhaps a more efficient method is the direct method in which the NMMO monohydrate is prepared first and then mixed with cellulose in a blender to form a solution. This method is not without fault either, however. Researchers found that if the cellulose solution is to have a concentration of more than 5 wt% and the NMMO is melted before the cellulose is added, forming a homogeneous solution can prove particularly difficult and require long mixing times [2, 20]. This problem can be worked around if the cellulose and NMMO are mixed at high speed and an elevated temperature below the melting temperature of NMMO. This allows the NMMO to diffuse into the cellulose and be uniformly mixed. Depending on the length of time and the temperature at which the mixing occurs, the resulting mixture may be a collection of granules or sticky slurry. Upon heating beyond the melting point, both the granules and the sticky slurry form a homogenous solution. The main difference between the two forms is the degree of preliminary penetration of the NMMO [2]. Since either form can be melted into a homogenous solution, the granules have the advantage of being less messy for transportation from a blender to an extruder if that is so desired.

3. Experimental Methods

A. Lyocell Preparation

Cellulose with an average DP of 670 was obtained in the form of paper sheets from Buckeye Technologies, Inc. Some of paper sheets were then broken into pieces and ground into a powder. The powder was then vacuum sealed in plastic bags until needed. A solution of 50-50 wt% NMMO and water, purchased from Huntsman Petrochemical Corporation, was dehydrated to make NMMO monohydrate. Lyocell solutions of 4, 6, 8, and 14 wt% cellulose were prepared from NMMO monohydrate, cellulose powder, and one percent by weight of cellulose of the antioxidant n-propyl gallate to prevent degradation of the cellulose at 90ºC and mixed at 80 rpm until transparent in a Brabender internal mixer. The length of time required for dissolution varied with concentration (Table 3). Immediately following solution preparation, an insignificant amount of particles were removed from the solutions by filtration. After cooling to a solid, the solutions were sealed in plastic bags. [20]

B. Differential Scanning Calorimetry

Lyocell samples were stored in reclosable freezer bags in a desiccator prior to use. To minimize the exposure of a sample to atmospheric moisture, the bags were

Table 3: Mixing time for the preparation of lyocell solutions.

Wt. % Cellulose	Mixing Time (hours)
4	1
6	1.5
8	3
14	4

subsequently transferred to a nitrogen rich glove bag environment where samples were transferred from their storage bags to DSC cells. The cells were sealed and transferred to a Perkin-Elmer Diamond differential scanning calorimeter (DSC) where a melting point analysis was performed with a heating rate of 15 ºC per minute. The sample bag was resealed in the nitrogen rich environment and subsequently returned to the dessicator. A minimum of seven runs for each concentration of lyocell were performed in this manner.

C. Thermogravimeteric Analysis

A small jar with a screw on lid was filled with approximately 300 mL of the 50% NMMO solution. From then on the jar remained sealed at all times except for brief periods when samples were removed. A syringe was used to transfer 5-25 mg of solution to a Pyris 1 TGA Perkin-Elmer thermogravimetric analyzer (TGA). The sample was heated at a rate of 20 ºC per min to 105 ºC and held steady at this temperature until the rate of weight loss in the sample was approximately zero.

Each concentration of lyocell was also run in the TGA in the same manner as the 50% NMMO solution. Lyocell samples were kept in sealed recloseable freezer bags which were stored in a desiccator. Lyocell samples weighing 1-10 mg were placed in the TGA with minimal exposure to the air. The samples were heated at a rate of 20 ºC per min to 105 ºC and held steady at this temperature for the duration of the sample run.

D. FTIR Spectroscopy

In order to obtain a mid-infrared profile of lyocell and perhaps use FTIR analysis as a non-destructive method for determination of cellulose concentration in unknown lyocell samples, cellulose fibers, NMMO monohydrate, and the four previously mentioned concentrations of lyocell were examined at room temperature with a Perkin-

Elmer Spectrum Spotlight FTIR Imaging System. Infrared images for the samples were obtained at wavelengths from 700 to 4000 cm^{-1} on 16 cm^{-1} intervals with 16 scans per pixel (Figure 5-7). The lyocell samples and pure NMMO monohydrate were heated and pressed into thin films between two potassium bromide (KBr) pellets and cooled to room temperature. So long as the films remained in between the pellets the NMMO monohydrate present in the sample could not absorb ambient moisture. Nine spectra from each infrared image resulting from the scans were analyzed using the Spotlight, Spectrum, and Unscrambler® software programs.

It was noted that the sides of the KBr pellets exposed to NMMO monohydrate became pitted. When the two KBr pellets were separated to remove the pure NMMO monohydrate or lyocell films, the films quickly absorbed moisture from the atmosphere so that drops of water were readily observed pooling on the film. It is well known that KBr is water soluble [21], so exposure to the liquid water likely began dissolving the surface of the pellets before it was cleaned off. It is unlikely that the KBr abstracted

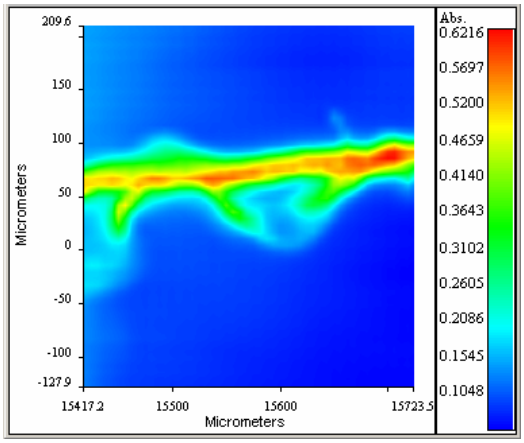

Figure 5: Infrared image of cellulose. Each pixel represents a full spectrum of absorbance data.

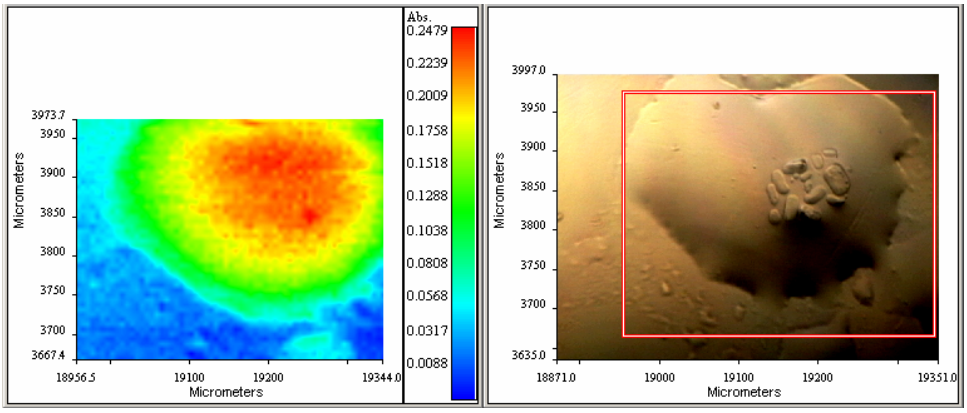

Figure 6: NMMO monohydrate drop and its infrared image. The box around the drop corresponds to the region where the infrared image was taken. Each pixel on the infrared image represents a full spectrum of absorbance data.

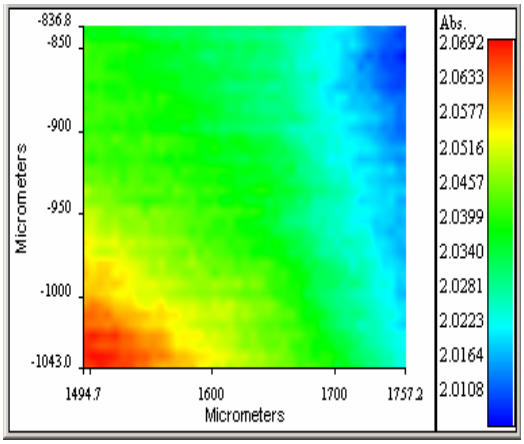

Figure 7: Infrared image of a 6% DP670 lyocell film. Each pixel represents a full spectrum of absorbance data.

water from the films because while KBr is also hygroscopic [21], its affinity for water is much less than that of NMMO monohydrate as evidenced by a lack of pitting on the external surfaces of the pellets exposed to NMMO monohydrate or on pellets exposed to only cellulose. It is also possible that the NMMO monohydrate, being an excellent solvent itself, dissolved part of the pellet surface. As a result of this pitting of the KBr pellets, zinc selenide (ZnSe) pellets were used for the remaining phases of the experiment and no pitting was observed.

The FTIR Imaging System was fitted with a hot stage that was temperature controlled to within 0.1ºC. Unfortunately, the hot stage did not allow enough room for the stacking of two pellets to seal NMMO-containing films against atmospheric moisture. As a result, a study was conducted to see at what temperatures spectra could be collected. Since the NMMO-containing films in the temperature study were not in a closed system, water could be absorbed onto the film and then desorbed with heating, preventing any meaningful determination of water content. However, before the NMMO used to make the films was exposed to the air, it was in the monohydrate form and was found to melt on the hot stage between 74 and 78ºC. It was determined that between 80 and 90ºC a quasi-equilibrium was reached such that water was not significantly absorbing onto the sample and thus changing the solubility of cellulose in the film, nor was the water driven off to the point of raising the melting point of the sample.

A median value of 85 ºC was initially chosen from the temperature study for collecting spectra on the hot stage. Then cellulose fibers and NMMO monohydrate were examined under the FTIR Imaging System. Next an attempt was made to observe the dissolution process with the FTIR Imaging System and hot stage. Cellulose fibers were

placed on a ZnSe pellet and brought into focus. Then NMMO monohydrate was added to the pellet as a solid and allowed to melt onto the fibers. Unfortunately this method tended to wash the fibers out of the area of focus on the stage. Since this generally prevented accurate measurements, the procedure was modified so that NMMO was first placed on a ZnSe pellet on the hot stage. After the NMMO had melted and the FTIR Imaging System focused on the liquid, cellulose fibers were added to the solvent. This could generally be directly in or very near the area of the stage already in focus so that little lateral adjustment was required and only slight adjustments to the focus were needed. Once the fibers were in focus, images and spectra could be collected. The first image and spectrum was usually collected within a minute of adding the fibers to the solvent. This method also had the added advantage of collecting a reference spectrum of NMMO before the fibers were added. The infrared measurements were taken at wavelengths from 700 to 4000 cm^{-1} on 8 cm^{-1} intervals with 16 scans per pixel. The spectra were then analyzed using the previously mentioned software.

E. Kinetic Study

During the course of the FTIR study it was noted that the series of images taken of the stage showed the gradual disappearance of cellulose fibers into the NMMO (Figure 8). It appeared that a visual method for observing the dissolution of individual cellulose fibers into NMMO had been developed. All the images taken on the FTIR hot stage were collected and analyzed using the ImageJ software program.

In an effort to automate the collection of dissolution images the hot stage was attached to an Olympus BS51 microscope to which a Scion Corporation CFW-1310C IEEE 1394 Firewire Color Digital Camera was attached. The camera was controlled

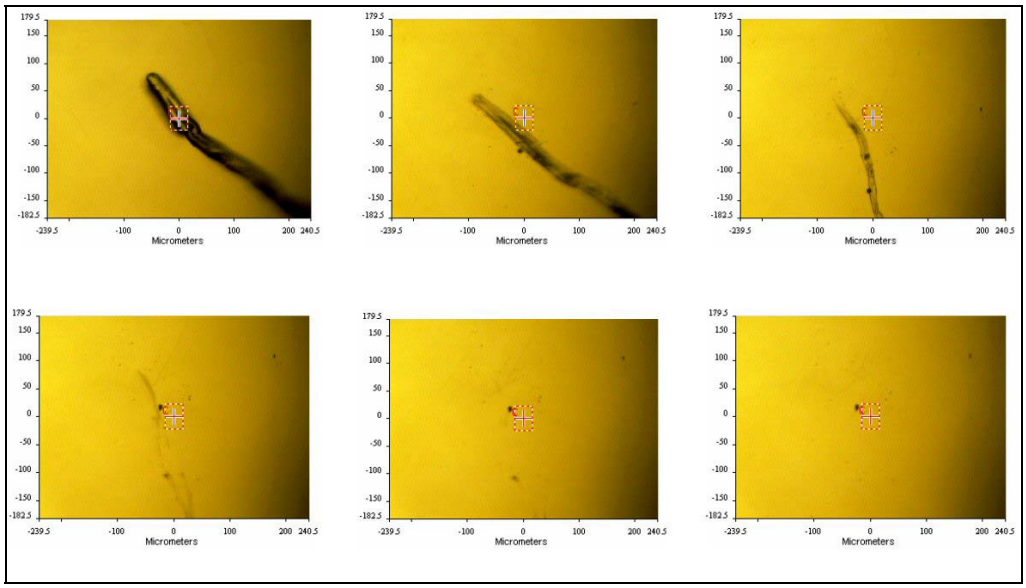

Figure 8: Series of images showing the dissolution of a cellulose fiber.

through the ImageJ software and was set to capture an image of a slide on the stage at a given intervals. The hot stage was set to 80, 85, or 90ºC. As in the FTIR study, obtaining results by placing cellulose fibers on a slide and adding NMMO proved extremely difficult. Although a few results with this method were obtained, adding fibers to already melted NMMO was found to be a more successful method. Once the fibers were added to the solvent, the camera was focused on a particular fiber or group of fibers. Then the camera was set to begin collecting images, which were stored on the attached computer. The resulting series of images, collectively referred to as a movie, were later analyzed with the ImageJ software.

In addition to capturing images of dissolving fibers, an image of a slide with standard increments was acquired and used to relate pixels on the computer to microns. The measurements from the software and the pixel to micron correlation were transferred to Microsoft Excel where the area measurements were converted to square microns.

4. Results and Discussion

A. Differential Scanning Calorimetry

A plot of heat flow vs. temperature was generated by the DSC from which melting point data could be extracted (Figure 9). The melting points were then plotted against cellulose concentration (Figure 10). Interestingly, the 6% lyocell sample showed a melting point nearly equal to that of the pure NMMO monohydrate sample. This does not fit the trend of decreasing melting point with increasing cellulose concentration. Strangely, the 4% and 8% lyocell samples also have similar values for the melting point of their respective samples.

Kim et. al. found that while the melting point of NMMO is depressed by cellulose, melting point depression in lyocell samples is more strongly dependent on water content [2]. Using this information one may infer that the average water content of the 6% lyocell samples was generally lower than the others and that the 4% and 8% samples had similar water content. Even though all the samples were made from monohydrate, they could have received varying exposures to moisture during preparation and transportation prior to testing. This inference was validated when this phenomenon was actually observed in one pure NMMO sample. The sample had, in some unknown fashion, been exposed to the atmosphere and had acquired water droplets on its surface that could be observed visually. A DSC scan of this hydrated sample showed a much wider peak than the other samples and a melting point that was two standard deviations below the average melting point of NMMO monohydrate, indicating a significant deviation from the mean. A sample need not have visually observable water droplets on its surface, however, to have absorbed enough moisture to affect its melting point.

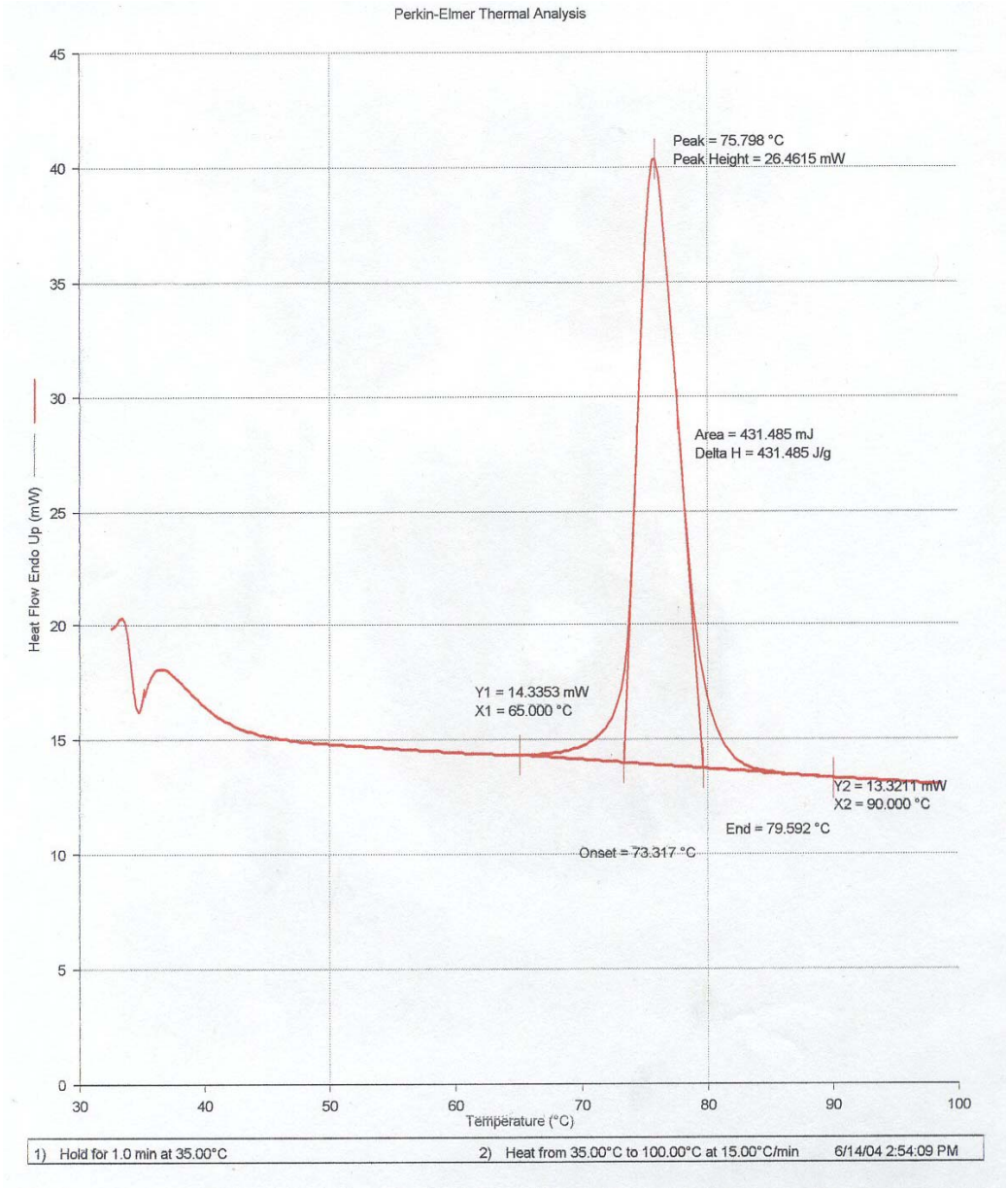

Figure 9: Example of a plot generated by the DSC. The peak shows the melting point of the sample.

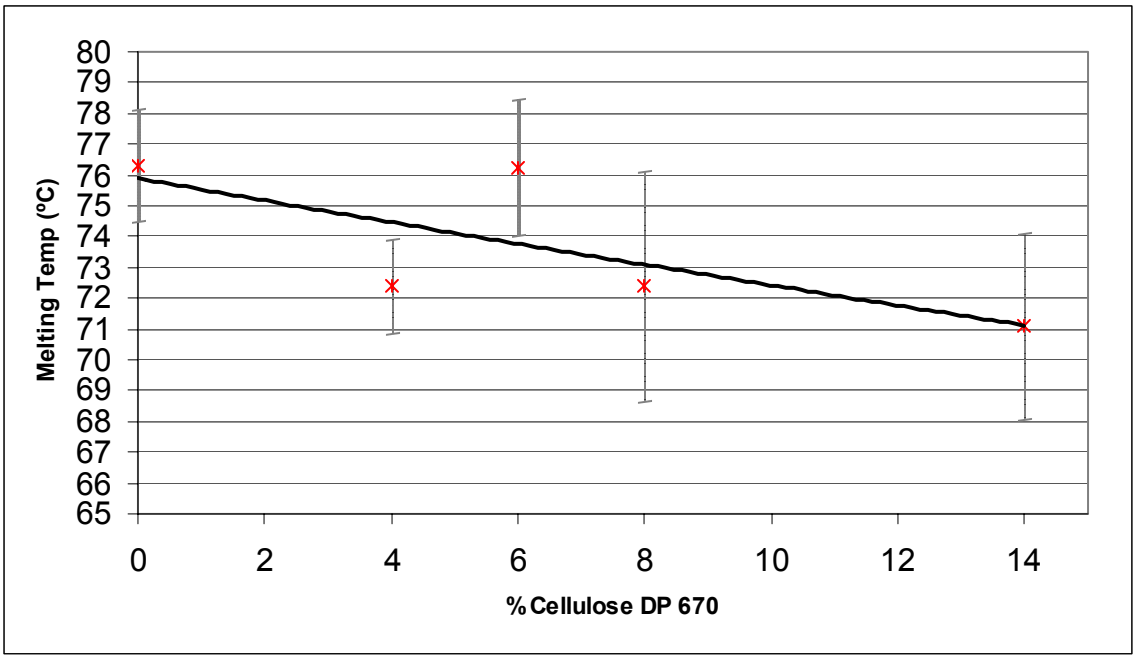

Figure 10: Average melting point of NMMO monohydrate vs. cellulose concentration.

This may also help to explain the larger standard deviations found in the lyocell samples, which inevitably received greater atmospheric exposure during the formulation than the NMMO monohydrate.

The literature also indicated a range of melting points for NMMO monohydrate. It was noted that things such as crystal size, scan speed, and type of DSC crucible could have an effect on the measured melting point [2, 8]. Although the results for NMMO monohydrate in this study fell within the specified literature values and the work generally supports that of other researchers, the fact that there is a range of accepted values coupled with the additional two factors of cellulose and water content that directly affect melting point led to the abandonment of further DSC testing for the purpose of developing a novel method for determining cellulose concentration [1, 2, 8, 22].

B. Thermogravimetric Analysis

A plot of wt% remaining versus time and its derivative was made for each sample run on the TGA (Figure 11). The plots of the 50-50 solutions have several distinct and interesting features. First, the maximum rate of evaporation is located at the minimum of the derivative, which is generally found in the first five minutes of a sample run and usually correlates to between 80 and 85 wt% of the sample remaining. The maximum evaporation rate is also found at the approximate point in time the sample reaches 100 ºC. One would expect the rate at which water is lost to be at a maximum at the boiling point of water, and then to decrease as the amount of water remaining decreases, which is observed in the plots of 50-50 wt% solutions.

However, the amount of water lost does not decrease uniformly. On the wt% remaining curve the water removal changes from an exponential decay to a linear decay and corresponds to a leveling off of the derivative curve. One might expect to find this change at the point the solution reaches the disesquihydrate phase, which is reached with about 69.2 wt% of the sample remaining. However, water is abstracted relatively easily from the disesquihydrate phase at elevated temperatures. The region between the disesquihydrate and monohydrate phases is a mixed phase containing both disesquihydrate and monohydrate and is where the transition from exponential to linear decay occurs. It is feasible that a less hydrated NMMO molecule may absorb some of the water molecules that are stripped off of the more hydrated NMMO molecules. The rate of this absorption increases as the concentration of the monohydrate increases resulting in an increased amount of time for an individual water molecule to be removed from the solution. The change to a linear decay could indicate the point were the absorption effect

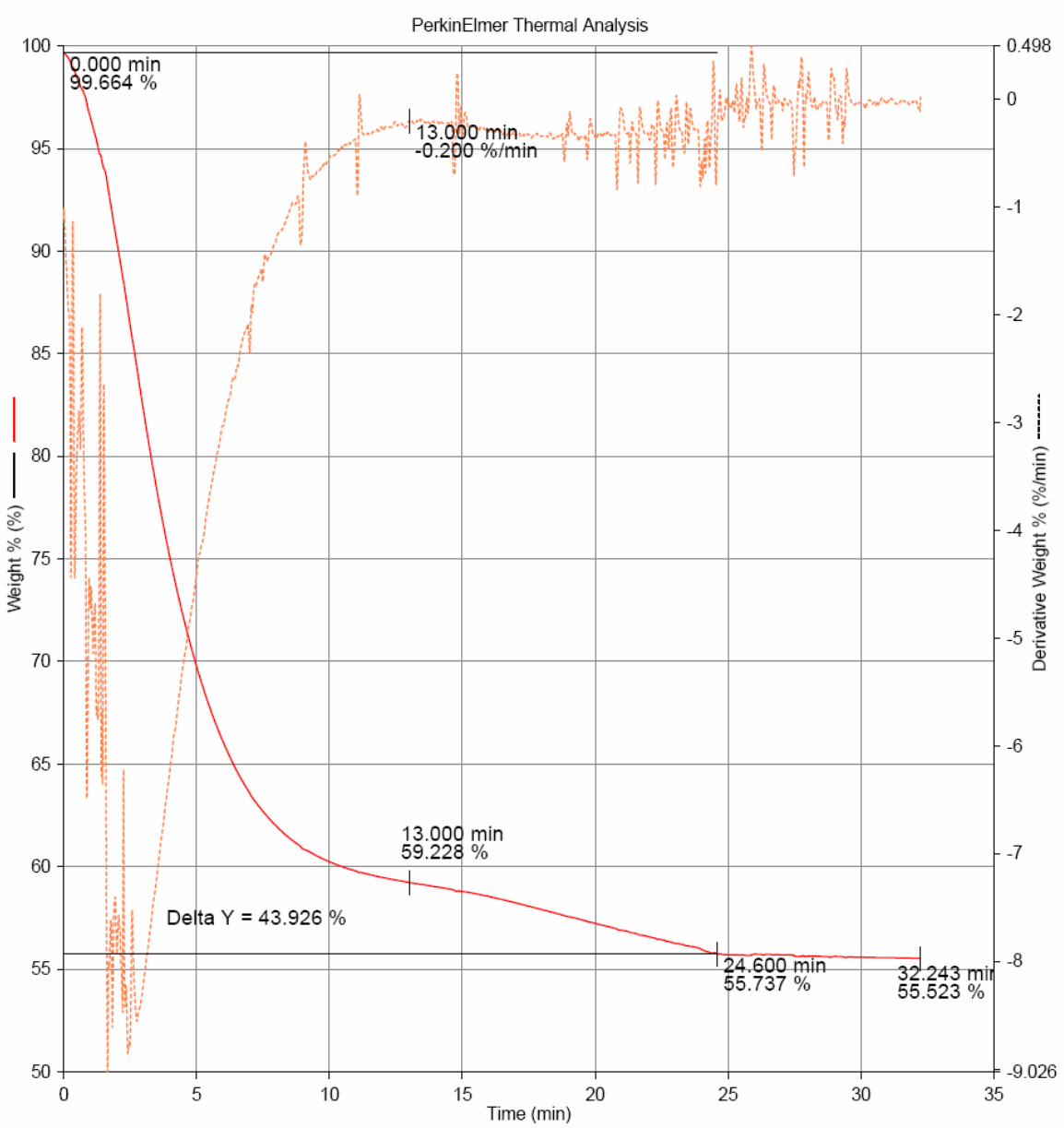

Figure 11: Example of a plot generated by the TGA. The solid red line shows wt% remaining versus time for a solution of 50-50 wt% NMMO and water while the dashed orange line shows the derivative.

becomes significant in the transport of the water in the removal process. Interestingly, this process appears to become significant near 59-61 wt% of the sample remaining, at which point the sample is approximately 16-18 wt% water, which is roughly the same composition as the onset of cellulose solubility in NMMO.

The second transition on the wt% remaining curve is a slope change that corresponds to the approximate location of the monohydrate phase of NMMO, which is reached with about 57.7 wt% of the sample remaining. Here the evaporation rate changes on the other side of the phase because the energy required to remove the water is greater. The water molecule attached to the NMMO in the monohydrate phase is bonded more strongly than the additional water molecules found in the disesquihydrate form, thus more energy is required to remove remaining water molecules.

It should be noted that in general, a larger percentage of water was removed from the 50-50 solution samples that were run earlier in the testing sequence. This is likely because as the vapor space above the liquid in the stock container increased, more water could evaporate from the solution slightly modifying the concentration. However, even assuming the initial water content is 50 wt% the second transition point is always near the monohydrate concentration. If one assumes that the second transition point is actually at the monohydrate concentration, the samples may be aligned by their transition point and the water content recalculated (Figure 12). The average water content found in the 50-50 solutions is shown in Table 4 and is slightly higher than 50 wt%. This is not particularly disturbing because manufacturers generally try to keep their product within certain specifications and not necessarily at precise levels. In fact, it is to a manufacturer's benefit to sell slightly more than 50 percent water since water obviously

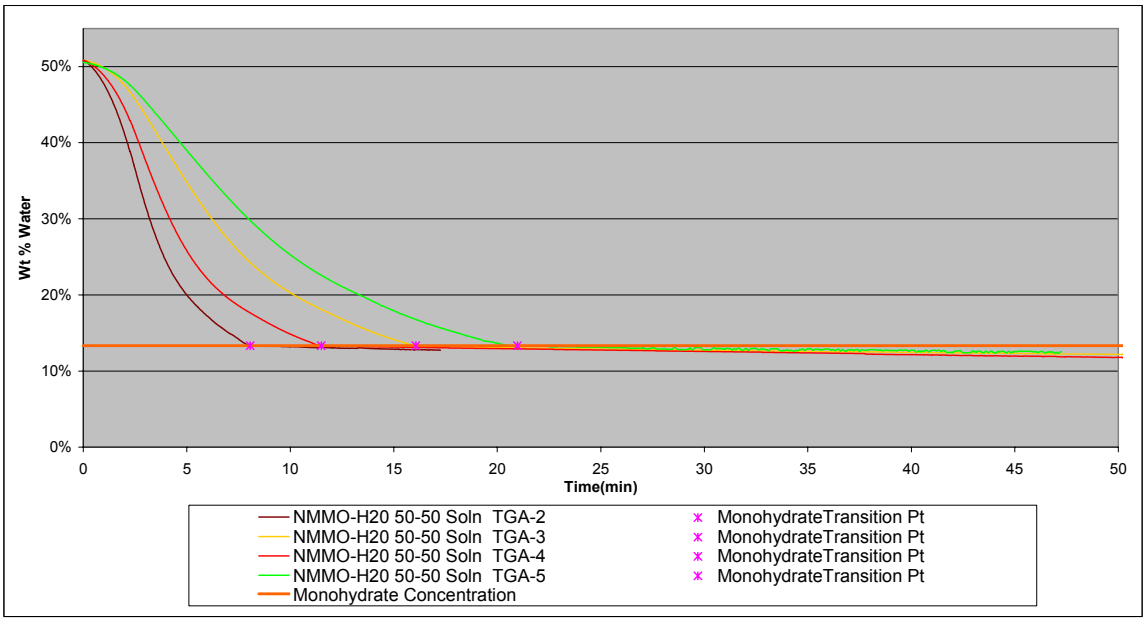

Figure 12: TGA data for some 50-50 solution curves aligned by their transition point. Each sample had a different initial mass, accounting for the horizontal spread, and was run according to the method described in Section 2.C

Table 4: Composite data for recalculated water content in 50-50 solutions.

Property	**Value**
Avg. Wt.% H_2O	50.625%
St. Dev.	0.680%
Max	51.680%
Min	49.540%
Range	2.140%

costs less than NMMO. Since the stock solution of NMMO appears to have been more than 50 percent water, the NMMO monohydrate samples used in other experiments, and the lyocell samples that were thought to have been produced from monohydrate likely have a hydration number larger than unity. This fact makes the development of a reliable method for determining water content in lyocell samples all the more important.

The water removal for lyocell is similar to that of the NMMO-water solution (Figure 13). However, there was only one significant feature on the weight percent remaining curve. This should be expected since the water content of the sample needed to be near the first slope change found in the 50 wt% water samples for the cellulose to be completely dissolved. The slope change is sometimes less distinct in the lyocell samples, perhaps allowing for the additional absorptive capacity of the cellulose, which, despite being only a fraction of the sample weight, contains many additional hydrogen bonding sites for the water molecules. Nonetheless, the lyocell samples show an approximately linear section on a plot of wt% remaining versus time which corresponds to a leveling off of the derivative curve. This is significant because it strongly resembles the monohydrate transition on the 50 wt% water samples in shape and slope. The lyocell samples appear to generally have a slightly smaller value for the slope, which may be due to the influence of the cellulose.

Assuming that the transition point on the lyocell samples is indeed at the monohydrate water concentration, then a simple back calculation using the amount of water lost may be used to determine the original water content and hydration number of the sample (Appendix B). If precautions are made to limit the exposure of the samples to air, running multiple samples from the same batch can confirm results and determine the

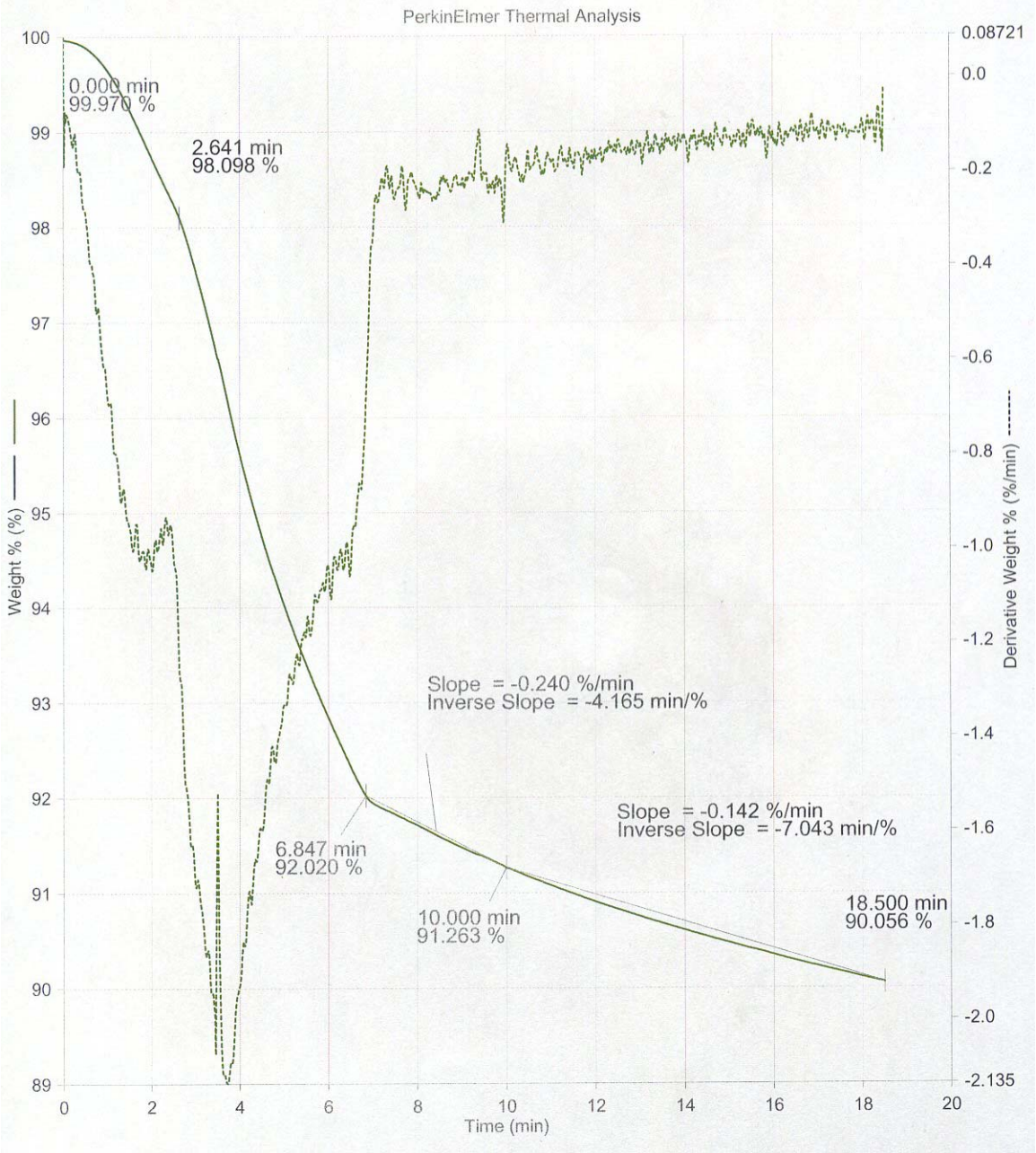

Figure 13: TGA plot for a lyocell solution containing 6% cellulose. The solid line shows wt% remaining versus time while the dashed line shows the derivative.

average water content for the batch of lyocell (Table 5). Unfortunately, this method will not work if the lyocell has a hydration number less than one, but since lyocell can be made above that hydration number and requires extra energy to go below the monohydrate concentration, the method should be applicable to most samples.

An interesting side note was discovered in the process of this experiment. When samples were stored in their sample bags in the desiccator for long periods of time the samples turned white. It appears that some of the water in the samples, despite being in sealed plastic bags, was removed by the desiccant, for which water apparently has a greater affinity. Another possible explanation is that after formulation and cooling to room temperature the samples crystallize over a long period of time, a behavior that has been observed for ionic liquids in a parallel study undertaken in this lab. However, the first explanation is somewhat more plausible because upon exposure to the atmosphere the samples absorb moisture from the air and are no longer white in a matter of minutes. Additionally, lyocell solutions identical to those stored in the desiccator did not turn white when stored in sealed plastic bags outside of a desiccator.

C. FTIR Spectroscopy

When this particular experiment was undertaken, it was known that spectra of cellulose and NMMO could show many similar peaks because NMMO and the cellulose repeat unit are largely composed of the same elements and have similar ring structures [13]. As such, it was desired to have some reference spectra for both cellulose and NMMO monohydrate so as to better understand the spectra collected from the lyocell solutions. Unfortunately reference spectra for NMMO monohydrate was rather difficult to obtain. Only one reference [23] was found, and it did not provide specific enough data

Table 5: Analysis of TGA results for lyocell samples.

Sample Wt (mg)	Wt% Cellulose	Wt% Remaining at Transition	Sample Hydration Number
9.826	4%	94.584%	1.44751
10.039	6%	95.490%	1.37697
5.311	8%	96.371%	1.30709
10.489	14%	91.30%	1.83132

for a quantitative comparison. Nonetheless, the paper did provide a point of reference for comparison, namely a series of peaks found between 1100 cm^{-1} and 1475 cm^{-1}. The Spectrum software was used to analyze the NMMO monohydrate spectra collected in the experiment and a similar profile to that found in the literature was noted (Figure 14). The peaks in Figure 14 are a result of the average of the spectra from multiple samples compiled by the software. The peaks of most significant interest are found at 1174, 1231, 1288, 1303, and 1368 cm^{-1}. Although the 1288 and 1303 cm^{-1} peaks sometimes merge due to their close proximity, the five peaks mentioned always show up strongly when mid-IR spectra are collected, making them key spectral identifiers for NMMO. When compared to the cellulose spectra (Figure 15), the peak at 1231 cm^{-1} of NMMO is of particular interest because there are no peaks for cellulose particularly nearby.

The cellulose spectrum shown can be deemed reliable because it closely resembled the spectra found in literature [24] and the IR database found in the Spectrum software. While cellulose itself was not in the database, ethyl cellulose was present and closely matched the samples. Unfortunately, the software did not have NMMO or any similar compounds in its database.

The various spectra collected on the lyocell and NMMO samples were imported into the Unscrambler® software for a principle component analysis (PCA) where a PCA

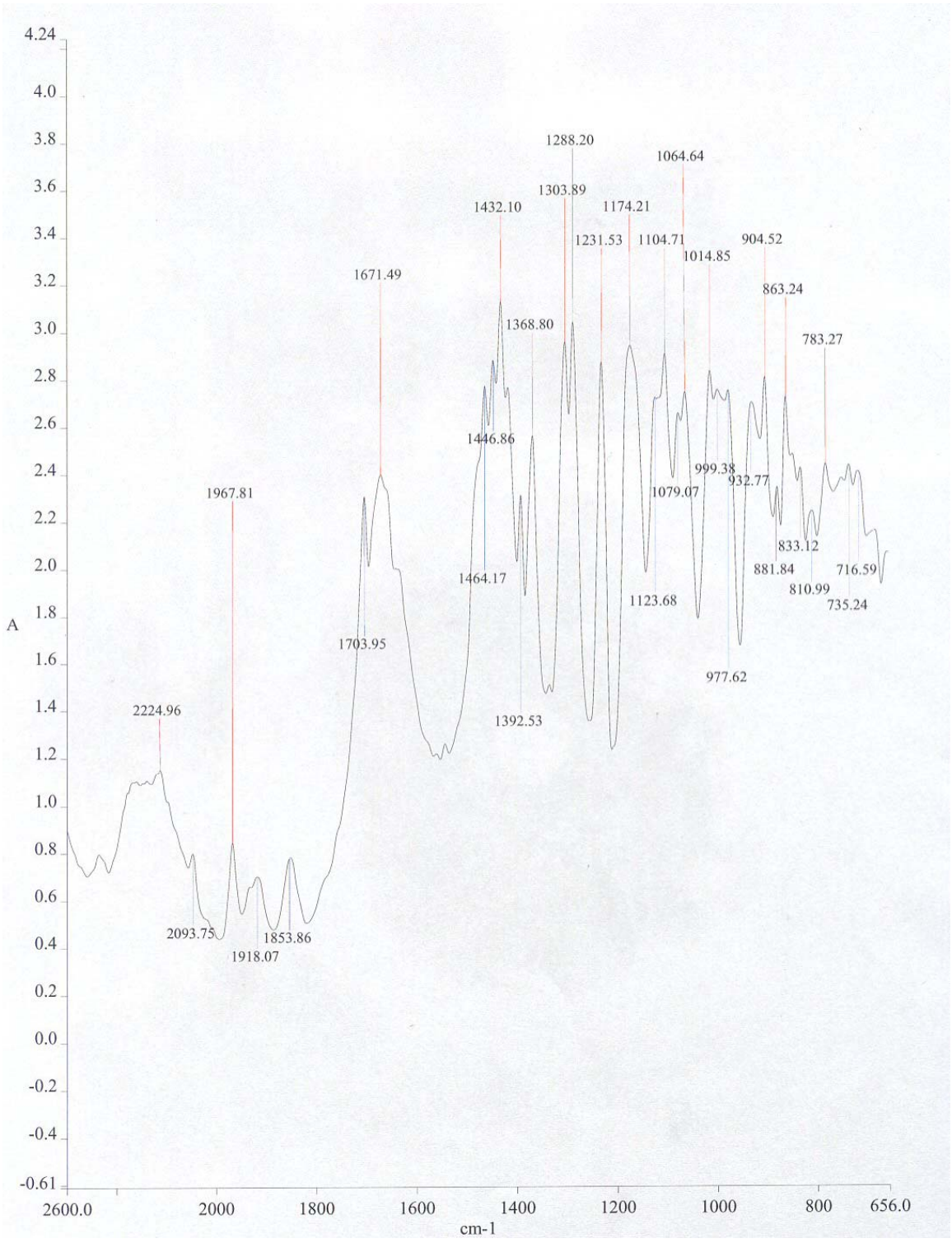

Figure 14: Average spectrum for NMMO samples. Series of distinguishing peaks between 1100 and 1475 cm^{-1}

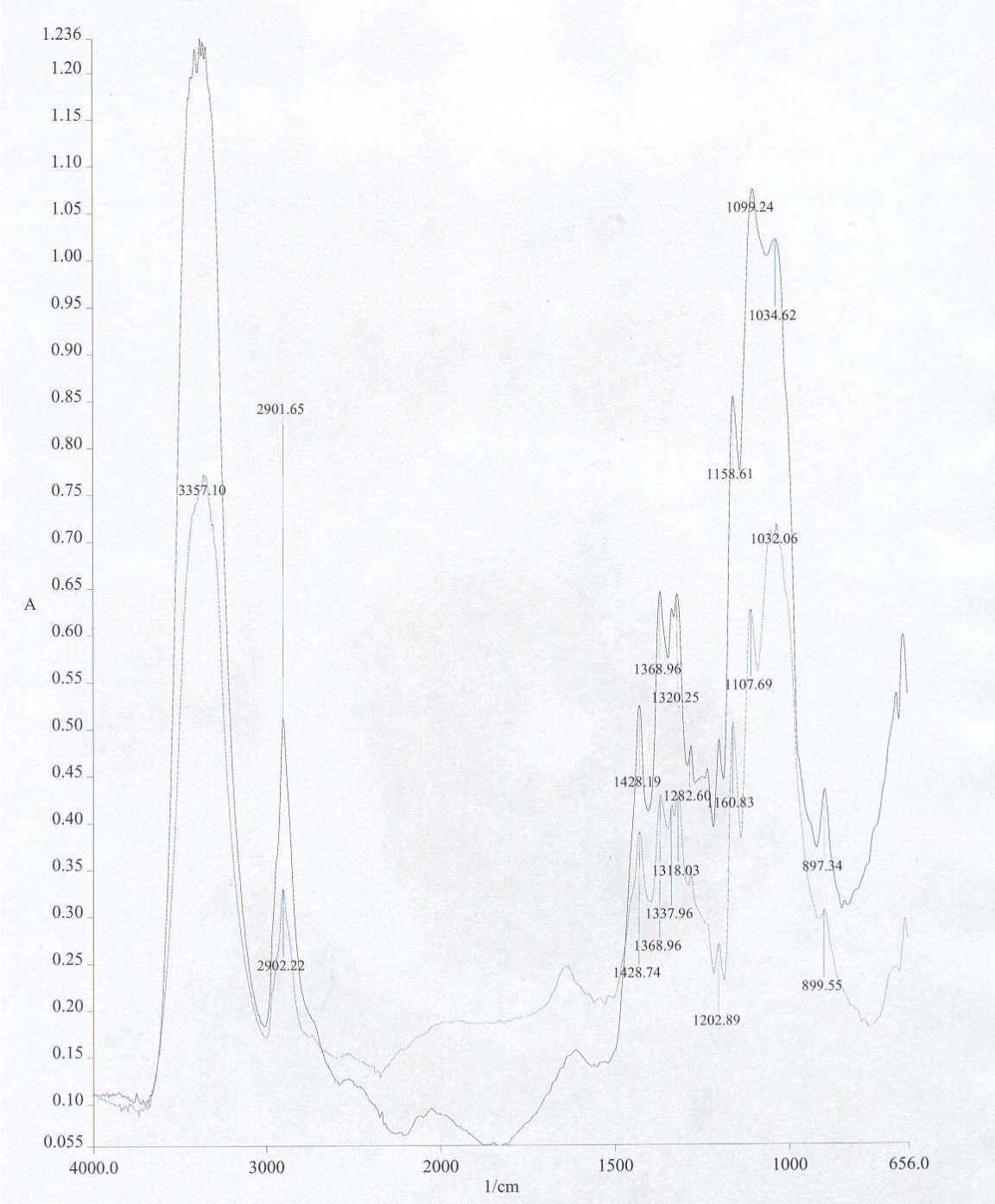

Figure 15: Spectra from two cellulose fibers. Cellulose fiber 5 (black). Cellulose fiber 6 (blue). Both matched the literature spectra for cellulose [24] and the IR database for ethyl cellulose. (Cellulose not in database)

plot was generated (Figure 16). Ideally, a PCA plot shows similar samples clustered together in distinct groups away from other clusters and the samples will fall in a recognizable pattern related to their concentration. The cellulose and NMMO monohydrate samples show good separation. The NMMO monohydrate samples also have a very tight cluster. Although the cellulose samples are rather spread out by comparison, some variation is expected due to the natural variation of the polymer. The lyocell samples did not cluster quite as well as the NMMO monohydrate, but the cellulose present in the lyocell solution again introduces some natural variation. All of the 4% cellulose spectra were eliminated by the software as outliers. This was not unexpected because the spectra collected from the 4% cellulose samples were noisy and showed poor resolution.

It was observed that the spectra from the 8% cellulose were particularly spread out, so their spectra were relabeled one, two, or three – based on which set of measurements the spectra came from. The 8% cellulose spectra were then found to be clustered nicely on this basis. The three separate clusters of the 8 % spectra show the variation that, while small in relation to the entire chart, is possible in infrared absorption, even among similar samples. Since all of the sample sets were treated in the same way, it is unlikely the variation among the 8% samples is a result of procedural or operational differences. However, the separation of the three clusters may suggest some inhomogeneity in the 8% solutions.

The 6 and 14 wt.% cellulose clustered relatively well without breaking them down by measurement set. The clustering of the lyocell samples away from the NMMO monohydrate spectra seems to indicate that adding cellulose to NMMO does indeed

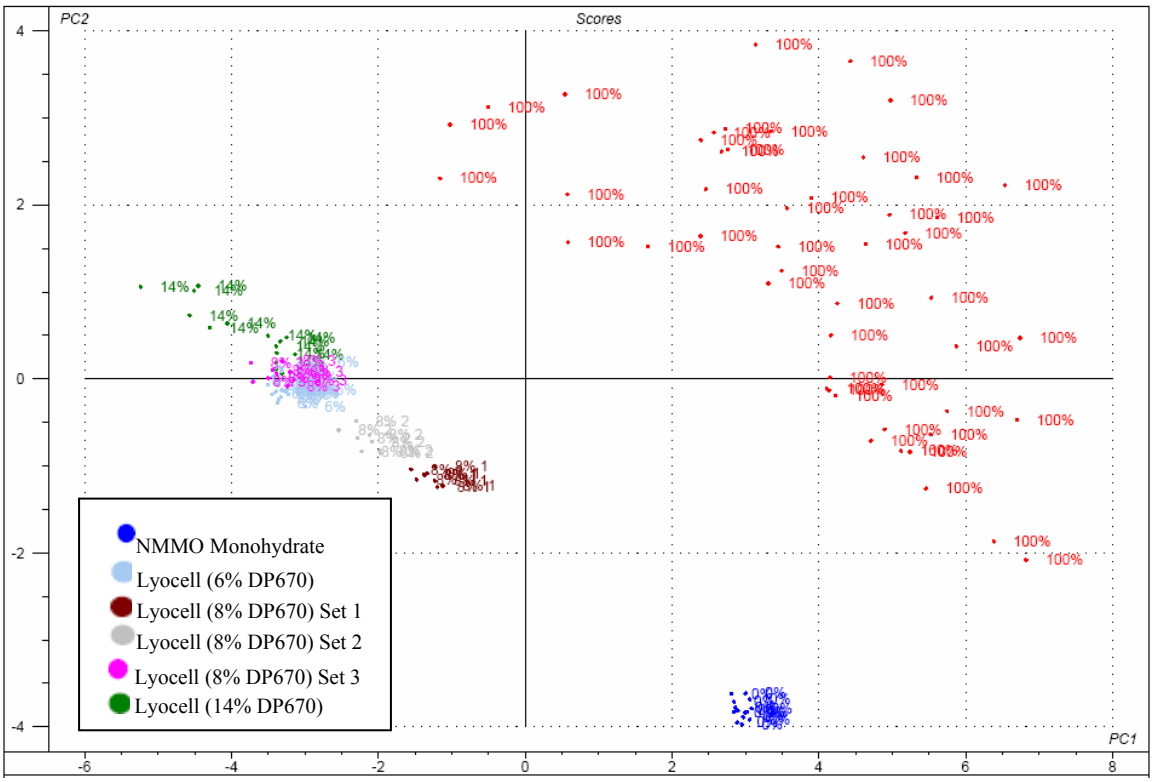

Figure 16: PCA plot of FTIR spectra.

change the way it absorbs infrared radiation. Unfortunately, the 6, 14 and one third of the 8 % spectra had some overlap in their respective clusters, suggesting a PCA may not necessarily be the most effective method for distinguishing cellulose concentration in lyocell solutions.

Recognizing the shortcomings in the PCA, a projection of latent structures (PLS) was undertaken on the full spectrum of the spectral data using the Unscrambler® software. Two-thirds of the data was randomly selected for the development of the PLS model. Since cellulose fibers are easily distinguishable from lyocell solutions by simple observation, and because there were no concentrations of cellulose between 14% and 100%, the fibers were excluded from the model. The PLS model (Figure 17) had a 98% data correlation and a root mean square error correction of 0.86% indicating a very good fit to the data. The regression coefficients for the model may be seen in Figure 18. The remaining one-third of the data was used to validate the PLS model (Figure 19). The model had an 89.8% correlation to the data and a root mean square error prediction (RMSEP) of 2.2%. It is expected that the model fits the calibration data more precisely than validation data because the model is developed from the calibration data. This means the model is essentially forced to fit the calibration data.

Interestingly, the model considers the 2600-2100 cm^{-1} region to be the region of most statistical significance, indicated by the height and width of the peak. However, cellulose and NMMO monohydrate do not have significant absorbance readings in this region. Additional PLS models were subsequently run using smaller portions of the infrared spectrum to see if a better model could be developed. The regions examined were 1530-700 cm^{-1} and 4000-2600 cm^{-1} due to the absorbance peaks these regions

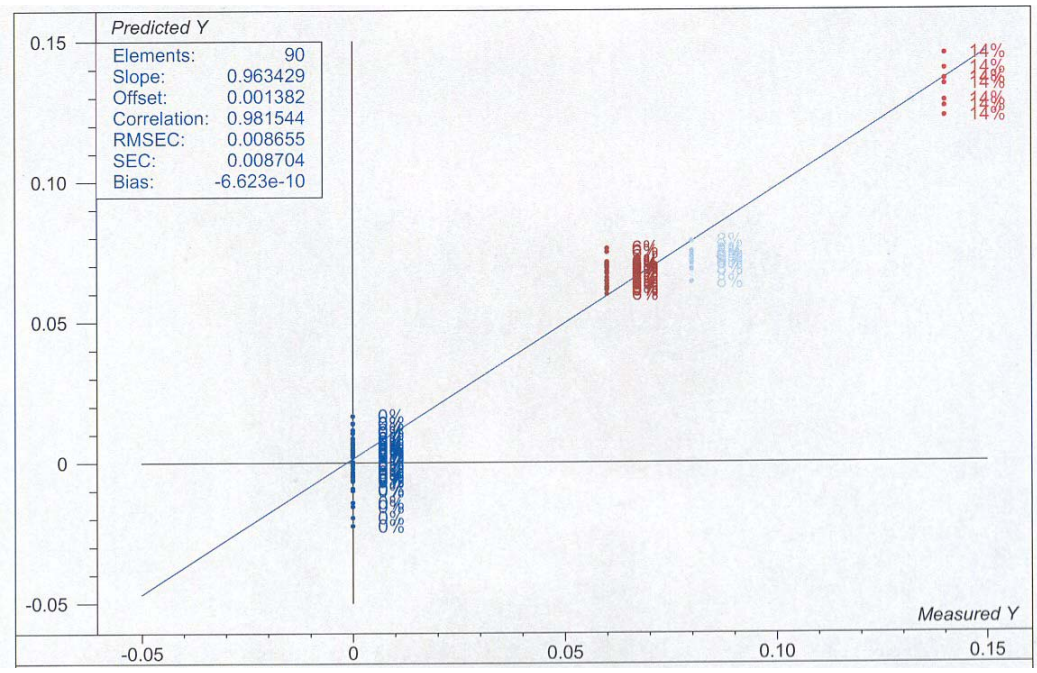

Figure 17: Calibration plot for PLS model utilizing the full spectrum.

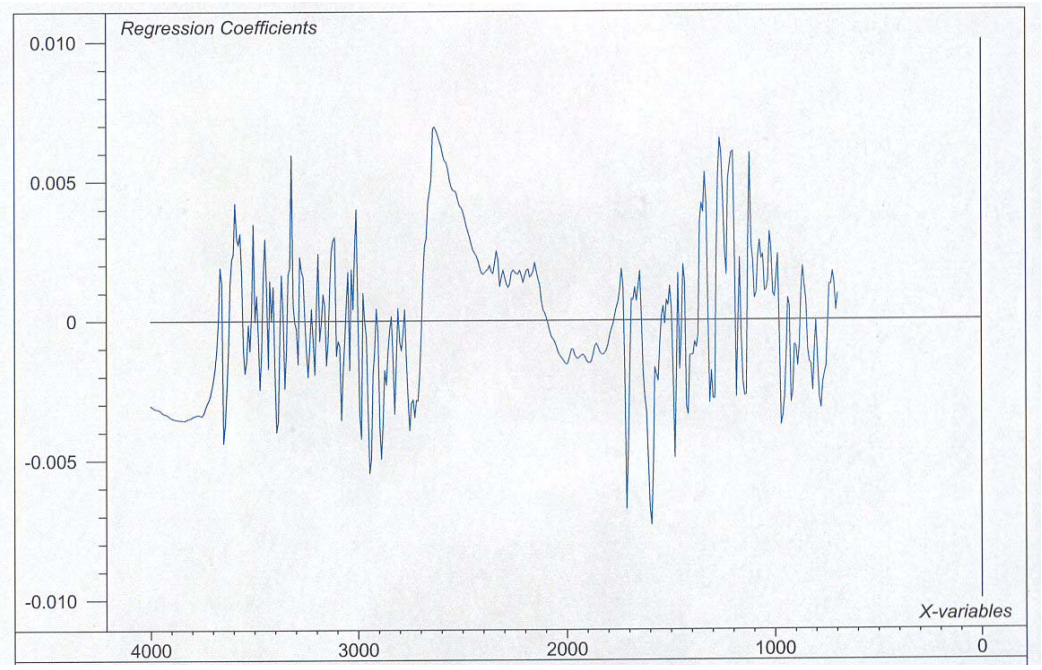

Figure 18: Plot of regression coefficients versus frequency. The PLS model utilizing these coefficients examined the full spectrum of data.

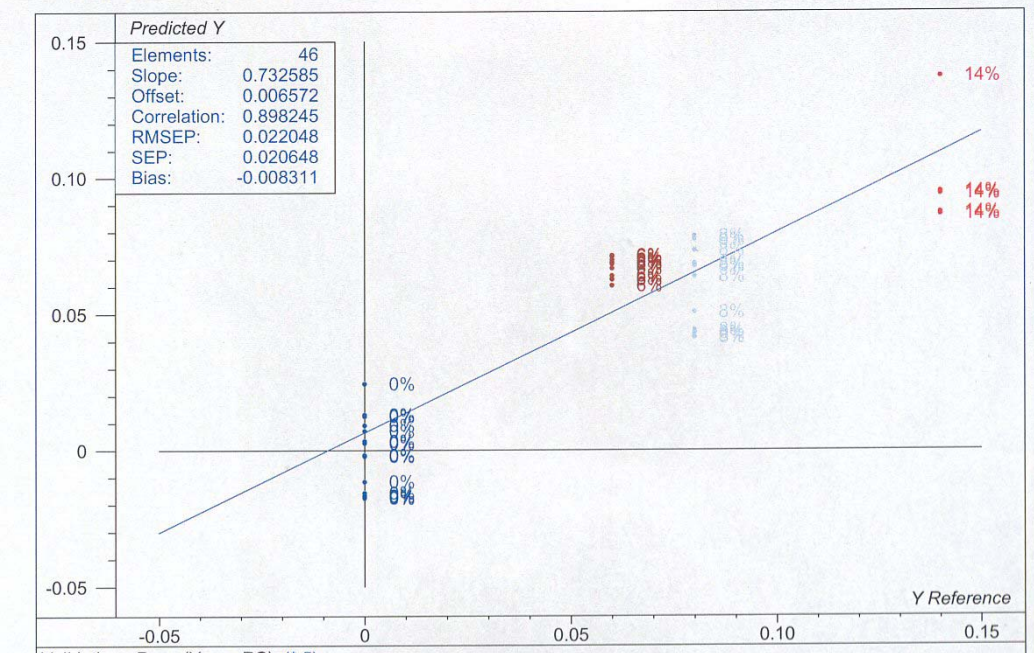

Figure 19: Validation plot for PLS model utilizing the full spectrum.

contain for NMMO monohydrate and celluose. A model for the 2600-1800 cm-1 region was also developed because of the significance assigned to it by the software. The results for the calibration of the models (Table 6) show that the original model gave the best correlation to the calibration data. However, when the additional models were validated, the results (Table 7) showed the 2600-1800 cm^{-1} and 1530-700 cm^{-1} models to have better correlation and smaller RMSEP than the original model when predicting the properties of the validation data. This clearly indicates that there are multiple regions of the spectrum that are significant in distinguishing the concentration of cellulose in lyocell solutions.

An interesting observation was made during the temperature study performed when the hot stage was attached to the FTIR Imaging System. When NMMO

Table 6: PLS calibration data.

Wavelength	Slope	Offset	Correlation	RMSEC
4000-700 cm^{-1}	0.963429	0.001382	0.981544	0.008655
1530-700 cm^{-1}	0.939965	0.002599	0.969518	0.001893
2600-1800 cm^{-1}	0.954495	0.00197	0.976983	0.010355
4000-2600 cm^{-1}	0.812100	0.008126	0.901166	0.021041

Table 7: PLS validation data.

Wavelength	Slope	Offset	Correlation	RMSEP
4000-700 cm^{-1}	0.732585	0.006572	0.898245	0.022048
1530-700 cm^{-1}	0.922820	0.001233	0.947140	0.015019
2600-1800 cm^{-1}	0.8519660	0.005506	0.958768	0.013607
4000-2600 cm^{-1}	0.7588780	0.014866	0.858324	0.023506

monohydrate was melted to form a thin film between 80 and 90ºC it appeared to neither quickly absorb water nor dehydrate. Apparently the degree of the hygroscopic nature of NMMO drops dramatically near the melting point of its monohydrate form. Perhaps a more likely possibility is that a pseudo-equilibrium between absorption and desorption is established where water is driven off at approximately the same rate as it is absorbed. This second line of reasoning seems more plausible because if the temperature is raised much above 90ºC, the film clearly begins to crystallize. The crystallization indicates a transition such that enough water has been desorbed from the film that the phase of the NMMO is dominated by the anhydrous form, which correlates to a higher melting point [8].

It was hoped that the infrared spectra taken during the dissolution of cellulose into NMMO on the hot stage would reveal something of the physiochemical process by which solvation of the cellulose occurs. In order for the cellulose fibers to dissolve in the film only a few fibers could be used because of the lack of shearing, which aids in the

breaking of the hydrogen bonds found in cellulose [1]. Thus, the concentration of cellulose was very small and its presence was masked in the infrared spectra by the excess of NMMO required for the dissolution of the fibers. Fortunately, this experiment led to a kinetic study and images gathered along with the spectra proved very useful in determining the rate constants of the dissolution. These results will be further discussed later.

These results seem to indicate that FTIR analysis may be an excellent way to qualitatively determine if a significant amount of cellulose is dissolved in NMMO. However, it appears that it may need to be refined as a technique for quantitative determination of cellulose content.

D. Kinetic Study

The ImageJ software allowed the area of the fibers in the collected images to be measured. The area of the fibers correlates directly to their concentration allowing the method of initial rates, as described by Fogler [19] and summarized in Section 2.E, to be used to determine the initial reaction rate from the area measurements (Figure 20). Some of the fibers did not immediately begin to decrease in area, so the method of initial rates was not applied until the decrease was observed. In the time prior to the area decrease, the fibers are still swelling and having hydrogen bonds broken. Once the hydrogen bonding sites have been freed from the intramolecular and intermolecular cellulose to cellulose bonding, the sites can begin attaching to the NMMO and thus dissolving the fiber into the solvent. This process of swelling and breaking the hydrogen bonds occurs more quickly in a stirred mixture because the shearing aids in mixing and breaking the hydrogen bonds in cellulose [1]. Additionally, some of the fibers in the study floated on

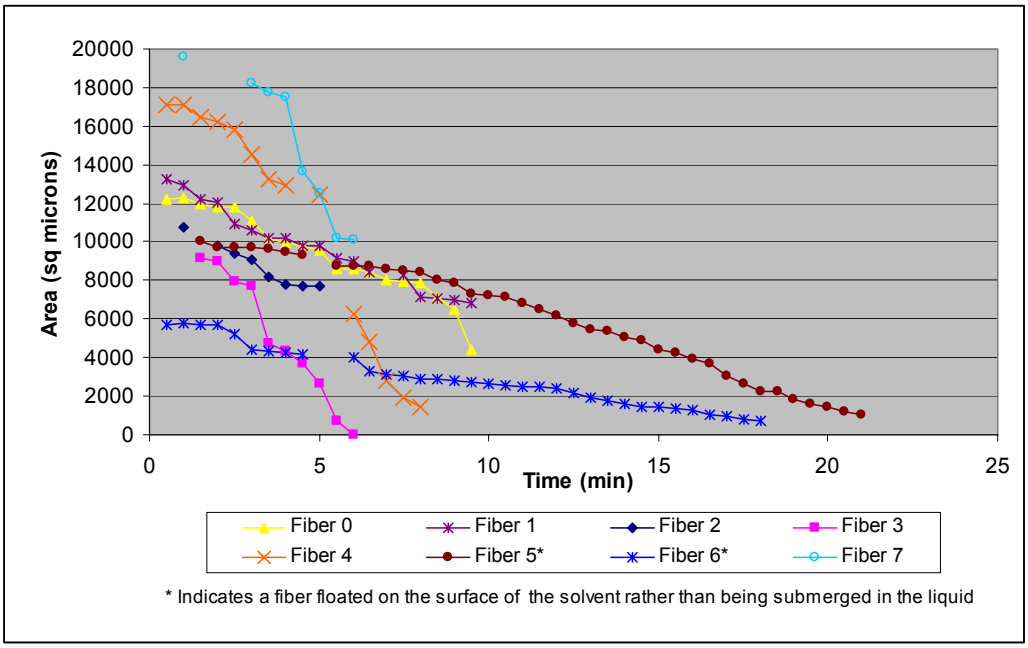

Figure 20: Dissolution measurements at 90ºC.

the surface of the solvent rather than being submerged in the liquid. The floating fibers received less exposure to the solvent and took longer to dissolve. Despite being a minority, the floating fiber data were included in the study and represent the effect fiber shape and folding can have on cellulose dissolution in NMMO monohydrate.

Once the initial rates were calculated for each movie using the method of initial rates, a plot of the natural log of the negative of the initial rate versus the natural log of the area was made for each temperature (Figures 21-23). The reaction order (a) and the natural log of the rate constant (k) could then be determined from each plot. Plotting the natural log of all three rate constants against the inverse of the temperature at which they were determined yields another plot (Figure 24) from which the pre-exponential factor (A) and activation energy (E) in the Arrhenius equation may be ascertained (Appendix A).

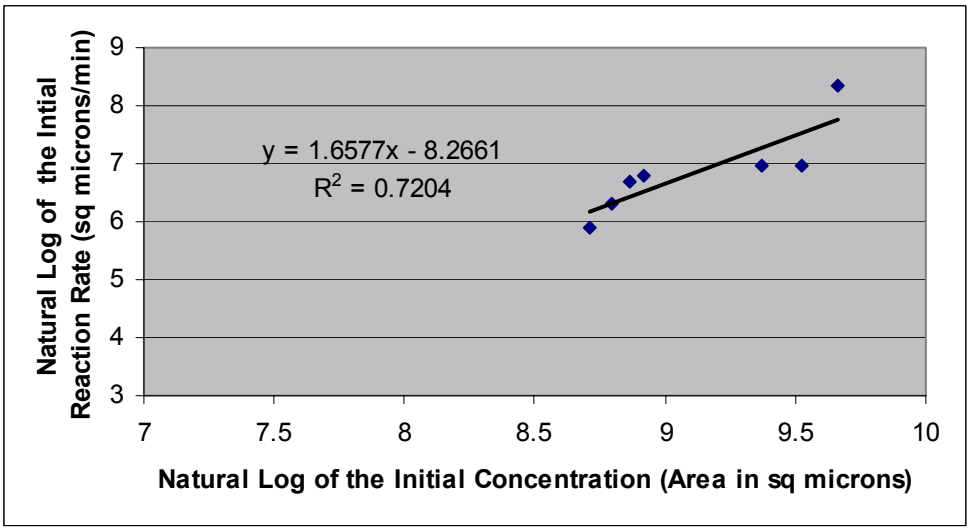

Figure 21: Kinetic data for cellulose dissolution at 80ºC.

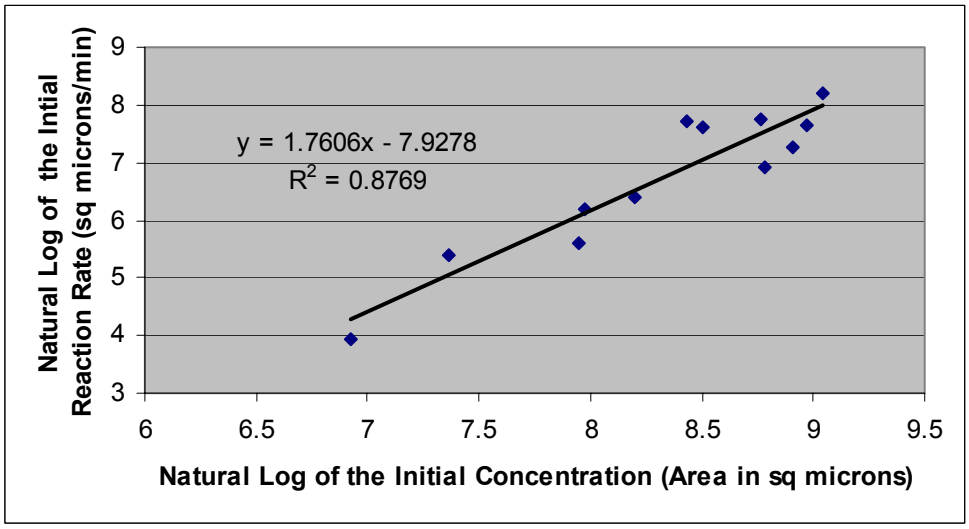

Figure 22: Kinetic data for cellulose dissolution at 85ºC.

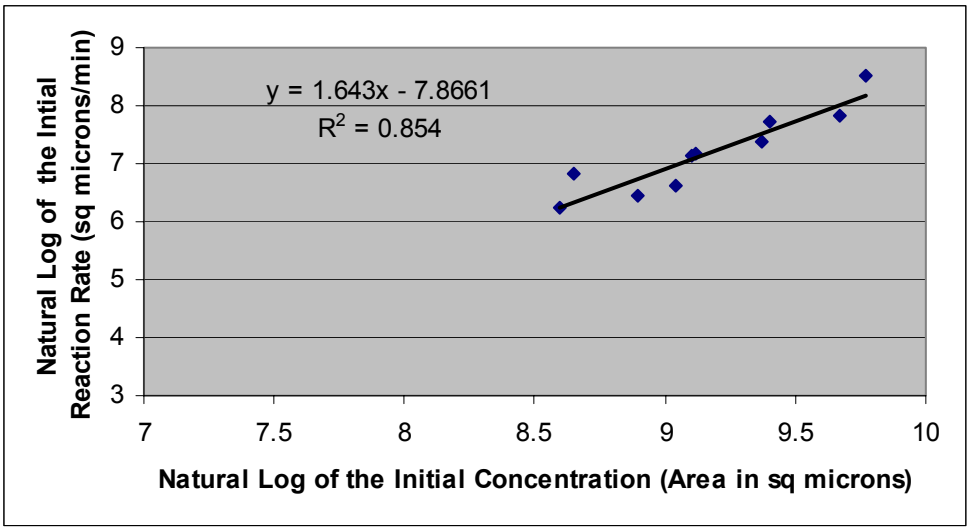

Figure 23: Kinetic data for cellulose dissolution at 90ºC.

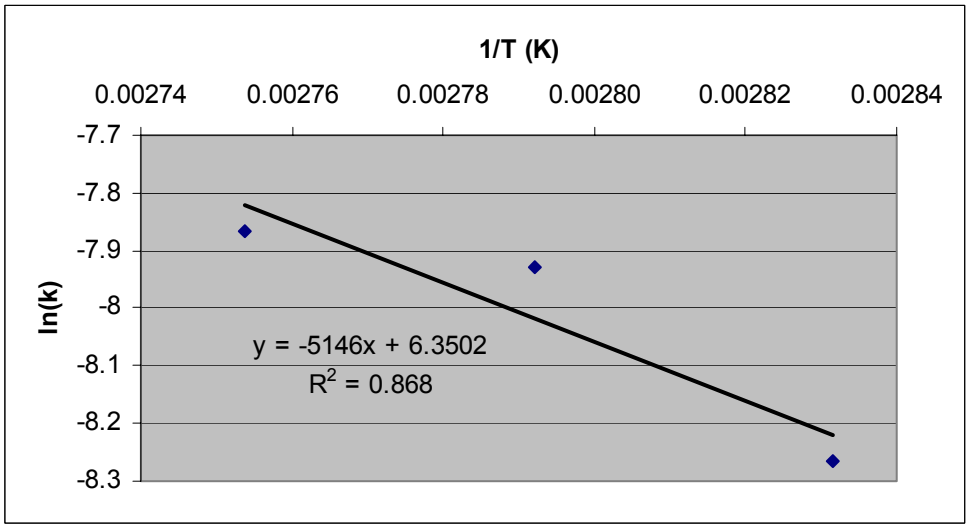

Figure 24: Arrhenius plot cellulose dissolution.

The kinetic data presented above clearly indicate the surface area and temperature dependence of cellulose dissolution into NMMO monohydrate, which encompasses the breaking and forming of hydrogen bonds and the diffusion NMMO monohydrate to less accessible regions of the cellulose, as described by Petrovan, et. al. The trend lines for the kinetic data presented above have a satisfactory variance and yield an Arrhenius plot with equally good variance with the rate constant at 85ºC trending slightly higher than the other two. The reaction order for the kinetic data at 85ºC is approximately seven percent higher than the other two, making it consistent with the rate constant. The final results from the kinetic study may be seen in Table 8.

Table 8: Results from kinetic study.

Temp (ºC)	a	k (μm^{-2})	A (μm^{-2})	E/R (K)
80	1.6577	0.000257	572.6	5146
85	1.7606	0.000361		
90	1.6430	0.000384		

5. Conclusions

In general, the DSC plot supports the work of other researchers [2, 8] who found that the melting point of NMMO is depressed with increasing cellulose concentration. Unfortunately, due to the number of factors influencing the melting point and the fact that they cannot all be isolated, DSC melting point analysis does not appear to be an effective method for determining cellulose concentration in lyocell solutions.

However, a thermogravimetric approach to determining the water composition of lyocell samples does appear effective. As water is evaporated from an NMMO or lyocell sample, there is a distinctive slope change where the hydration number is one. Using TGA data, a simple back calculation may be performed to get the initial concentration of water in the sample. Additionally, a slope change in the rate of evaporation may be observed near 16-18 wt% water in an NMMO sample. The slope change is significant because of its proximity to the region where cellulose solubility begins when NMMO is the solvent. The water-NMMO interactions at this ratio may bear further examination. Notably, cellulose appears to slow the evaporative process in lyocell relative to pure NMMO samples due to large capacity of cellulose for forming hydrogen bonds.

Detailed mid-infrared spectra of NMMO monohydrate and cellulose were obtained. Mid-infrared spectra were also obtained for several concentrations of lyocell, which were then analyzed using PCA and PLS to determine if FTIR analysis could distinguish between varying concentrations of cellulose in lyocell solutions. The PCA showed distinct and separate clusters for NMMO monohydrate and lyocell solutions, however, some of the different concentrations of lyocell solutions overlapped. This indicates that FTIR analysis coupled with PCA may be an excellent way to qualitatively

determine if a significant amount of cellulose is dissolved in NMMO, but it may need to be refined as a technique for quantitative determination of cellulose content. The predicative model from the PLS on the FTIR spectra more clearly distinguished between the various concentrations of lyocell and shows great potential for being a quantitative determination of cellulose content. The specific regions of the spectrum most significant to such a quantitative determination have not yet been fully identified, but it has been clearly shown that multiple regions are important.

Observations of a thin film of NMMO monohydrate on a hot stage indicate that raising the temperature of the thin film above approximately 90ºC will cause it to solidify. Additionally, it was noted that NMMO monohydrate and lyocell solutions should not be used in conjunction with KBr pellets due to the hygroscopic nature of NMMO monohydrate which results in the pitting of the pellet surface. Instead a more chemically inert, water insoluble pellet, such as ZnSe, should be used.

The swelling processes during cellulose dissolution discussed by other researchers were observed. The surface area and temperature dependence of the process of cellulose dissolution into NMMO monohydrate were clearly demonstrated. The rate constant, pre-exponential factor, and activation energy for cellulose dissolution in NMMO monohydrate were also determined (Table 8).

Future work might include an examination of the phase behavior of NMMO at the onset of cellulose solubility and a DSC analysis of the crystallization of lyocell samples to aid in understanding the dissolution process. A more detailed multivariate analysis of mid-infrared spectra from lyocell solutions may also be performed in the future to refine the PCA and improve the PLS predictive model.

References

References

1. Roesnau, T; Potthast, A; Sixta, H; Kosma, P. "The Chemistry of Side Reaction and Byproduct Formation in the System NMMO/Cellulose (Lyocell Process)." *Progress in Polymer Science.* Vol. 26 2001 p.1763-1837
2. Kim, D.B.; Jo, S.M.; Lee, W.S.; Pak, J.J. "Physical Agglomeration Behavior in Preparation of Cellulose-N-Methyl Morpholine N-oxide Hydrate Solutions by Simple Mixing." *Journal of Applied Polymer Science*. Vol. 93 2004 p. 1687-1697
3. Adorjan, I.; Sjöberg, J; Rosenau, T; Hofinger, A.; Kosma, P. "Kinetic and Chemical Studies on the isomerization of monosaccharides in N-methylmorpholine-N-oxide (NMMO) under Lyocell conditions." *Carbohydrate Research.* Vol. 339 2004 p. 1899-1906
4. Rosenau, T; Hofinger, A.; Potthast, A; Kosma, P. "On the Conformation of the Cellulose Solvent N-Methylmorpholine-N-oxide (NMMO) in solution." *Polymer.* Vol. 44 2003 p. 6153-6158
5. Kim, S.O.; Shin, W.J.; Cho,H. Kim, B.C.; Chung, I.J. "Rheological Investigation on the Anisotropic Phase of Cellulose-MMNO/H20 Solution System." *Polymer. Vol.* 40 1999 p.6443-6405
6. Kim, D.B.; Lee, W.S.; Jo, S.M.; Lee, M.L.; Kim, B.C. "Effect of Thermal History on the Phase Behavior of N-Methyl Morpholine N-oxide Hydrates and Their Solutions of Cellulose." *Polymer Journal* Vol. 33 2001 p. 139-146
7. Chae, D.W.; Kim, B.C.; Lee, W.S; "Rheological Characterization of Cellulose Solutions in N-Methyl Morpholine N-Oxide Monohydrate." *Journal of Applied Polymer Science.* Vol.86, 2002 p. 216-222
8. Chanzy, H.; Nawrot, S.; Peguy, A; Smith, P. "Phase Behavior of the Quasiternary System N-Methylmorpholine-N-Oxide, Water, and Cellulose." *Journal of Polymer Science.* Vol. 20, 1982 p. 1909-1924
9. Shimizu, T.; Furukawa, Y.; "Method of detecting electrode potential in Karl Fischer moisture meter." United States Patent 4664756. Filed: 1984-12-27. Published: 1987-05-12.
10. Niekraszewicz, B.; Czarnecki, P. "Modified Cellulose Fibers Prepared by the N-Methylmorpholine N-Oxide (NMMO) Process." *Journal of Applied Polymer Science.* Vol.86, 2002 p. 907-916
11. Lim, K.Y.; Yoon, K.J.; Kim, B.C. "Highly Absorbable Lyocell Fiber Spun from Cellulose/Hydrolyzed Starch-g-PAN solution in NMMO monohydrate." *European Polymer Journal.* Vol. 39 2003 p. 2115-2120
12. Suñol, J.J.; Saurina, J.; Carrillo, F.; Colom, X. "Comparison of the Thermal Behavior of Three Cellulose Fibers Mercerized or Submitted to Solar Degradation." *Journal of Thermal Analysis and Calorimetry.* Vol. 72, 2003 p.753-758
13. Marhöfer, R.J.; Kast, K.M.; Schilling, B; Bär, H.J.; Kast, S.M.; Brickmann, J. "Molecular dynamics simulations of tertiary systems of cellohexaose/aliphatic N-oxide/water." *Macromolecular Chemistry and Physics*, Vol. 201 2000 p. 2003-2007

14. Kast, K.M.; Reiling,S.; Brickmann, J. “Ab initio investigations of hydrogen bonding in aliphatic N-oxide–water systems.” *Journal of Molecular Structure (Theochem).* Vol. 453, 1998 p. 169–180
15. Laity, P.R.; Glover, P.M.; Hay, J.N.; ”Composition Phase Changes Observed by Magnetic Resonance Imaging During Non-solvent Induced Coagulation of Cellulose.” *Polymer*. Vol. 43 2002 p.5827-5837
16. Rosenau, T; Potthast, A; Milacher, W.; Hofinger, A.; Kosma, P. “Isolation and Identification of Residual Chromophores in Cellulosic Materials.” *Polymer.* Vol. 45 2004 p. 6437-6443
17. Petrovan, S.; Negulescu, I.; Collier, J. “Elongational and Shear Rheology of Cellulosic and Lignocellulosic Solutions in N-Methylmorpholine Oxide Monohydrate.” *Cellulose Chemistry and Technology* Vol. 35 2001 p. 89-102
18. Kast, K.M.; Brickmann, J.; Kast, S.M.; Berry, R.S. “Binary Phases of Aliphatic N-Oxides and Water: Force Field Development and Molecular Dynamics Simulation.” *Journal of Physical Chemistry A*. Vol. 107 2003 p. 5342-5351
19. Fogler, H.S. *Elements of Chemical Reaction Engineering*. 3rd ed. Upper Saddle River, NJ: Prentice Hall, 1999.
20. Li, Zuopan. “Rheology of Lyocell Solutions from Different Cellulosic Sources and Development of Regenerated Cellulosic Microfibers” PhD Dissertation, The University of Tennessee. August 2003.
21. Lide, D.R., ed. *CRC Handbook of Chemistry and Physics.* 80th ed. New York City, NY: CRC Press, 1999
22. Navard, P.; Handin, J.M. “Thermodynamic Study on N-methylmorpholine N-oxide.” *Journal of Thermal Analysis.* Vol. 22, 1981 p. 107
23. Shimizu, T.; Furukawa, Y.; “Method of detecting electrode potential in Karl Fischer moisture meter.” United States Patent 4664756. Filed: 1984-12-27. Published: 1987-05-12.
24. Oh, S.Y.; Yoo, D.I.; Shin, Y.; Seo, G. “FTIR analysis of cellulose treated with sodium hydroxide and carbon dioxide.” *Carbohydrate Research.* Vol. 340, 2005 p. 417-428

Appendices

Appendix A: Kinetic Equations

r =reaction rate
k =reaction rate constant
C =concentration of reactant
a =reaction order
E =activation energy in Arrhenius Equation
A =pre-exponential factor in Arrhenius Equation
R =ideal gas constant

Rate law: $-r = k \cdot C^a$

$\ln(-r)=\ln(k) + a \cdot \ln(C)$

Arrhenius Equation: $k= A \exp(-E/(R\ T))$

$\ln(k) = \ln(A) – (E/R)(1/T)$

Appendix B: Equations for Back Calculation of Water Content from TGA Data

M_o = initial mass of sample
M_c = mass of cellulose in sample
M_t = mass of sample at transition point
M_{mh} = mass of monohydrate at transition point
X = wt% remaining at transition point (from TGA Data)
X_c = wt% cellulose in sample
X_{w0} = initial weight fraction of water in the sample
N_s = millimoles of NMMO
N_w = millimoles of water at transition point
N_{lost} = millimoles of water lost
N_{w0} = intial millimoles of water
MW_w = molecular weight of water = 18.0152 mg/millimoles
MW_s = molecular weight of NMMO = 117.1474 mg/millimoles
TR = transition ratio of millimoles of NMMO to millimoles of water (usually 1)
n = hydration number

$$N_w = \frac{M_o (X) (1-X_c)}{MW_w + TR (MW_s)}$$

$$N_{lost} = (1-X) M_o (MW_w)^{-1}$$

$$N_{w0} = N_w + N_{lost}$$

$$N_s = \frac{M_o X (1-X_c)}{MW_s + MW_w (TR)^{-1}}$$

$$n = N_w (N_s)^{-1}$$

$$X_{w0} = (N_{w0}) (MW_w) (M_o^{-1})$$

Vita

John William Tierney was born in 1980 and grew up in the small mining community of Viburnum, MO. After graduating from high school in 1999, he attended the University of Missouri-Rolla where he met and married the love of his life, Melinda. Upon graduation from UMR in December of 2003 with a B.S. in Chemical Engineering and a minor in Chemistry, John moved to Knoxville to continue his education at the University of Tennessee. In December 2005, John earned a Master of Science degree in Chemical Engineering.